DANMARKS OG GRØNLANDS GEOLOGISKE UNDERSØGELSE RAPPORT 2012/121

Review and evaluation of gravity data from Gosetal, Harz Mountains, Germany

Report prepared for Scandinavian Highlands Holding A/S

T. M. Rasmussen

GEOLOGICAL SURVEY OF DENMARK AND GREENLAND
DANISH MINISTRY OF CLIMATE, ENERGY AND BUILDING

GEUS

DANMARKS OG GRØNLANDS GEOLOGISKE UNDERSØGELSE RAPPORT 2012/121

Review and evaluation of gravity data from Gosetal, Harz Mountains, Germany

Report prepared for Scandinavian Highlands Holding A/S

T. M. Rasmussen

(1 DVD included)

Released 01.01.2018

GEOLOGICAL SURVEY OF DENMARK AND GREENLAND
DANISH MINISTRY OF CLIMATE, ENERGY AND BUILDING

GEUS

Contents

1. Executive summary

Gravity data reported previously by Plaumann (1971) from the Gosetal area are analysed with the objective of identifying locations with mineralisations similar to those at the Rammelsberg mine. The data processing performed by Plaumann is verified and extended based on new topographic terrain corrections. Moreover, a regional-residual anomaly separation is performed in order to obtain data for modelling.

Three residual gravity anomalies are identified and evaluated to be of interest in a search for mineralisations. One of these anomalies is co-located with a low resistivity structure identified by an electromagnetic SkyTEM survey. This anomaly is furthermore coincident with an anomaly in soil-gas. The gravity anomaly is modelled using a dense tabular body dipping towards south-east.

The main conclusion from the modelling is that the gravity data do not exclude the presence of an ore body below the SkyTEM anomaly. It is furthermore concluded that the observed gravity anomaly is unlikely to be caused by erroneous correction for topographic effects.

In order to add more confidence to the interpretation of the gravity data, density information on both host rocks and presumed mineralisation are required. Improvements are also possible by denser gravity station spacing. Preferentially, density information from rocks samples collected along gravity station profiles should be obtained.

2. Introduction

An airborne electromagnetic survey with the SkyTEM system (SkyTEM ApS, 2009) revealed a low resistive anomaly in Gosetal, approximately 2 kilometres west of the historic Rammelsberg mine in the Harz Mountains of Germany. The Rammelsberg mine contained a world class, massive sulphide, SEDEX-type base metal deposit. The resistivity anomaly is therefore considered an obvious target in a search for similar types of mineralisations. Drilling within the anomalous zone has so far not revealed the cause of the observed anomaly. Therefore, existing gravity data (Plaumann, 1971) was selected for re-evaluation in order to provide complementary information about a possible mineralisation. In this report, particular focus is given the following points:

- the terrain corrections performed on the gravity data,
- identification of target anomalies for modelling and further investigation,
- modelling of a gravity anomaly co-located with the resistivity anomaly
- suggestions for further investigations

3. Data and maps

This chapter contains a presentation of various types of data available from the survey area.

3.1 Geology

The crustal structure around the Harz Mountains is reviewed in Brink (2011) and the mineralisation at the Rammelsberg mine is described by Mueller (2008) in the SGA Webb Mineral Deposit Archive (www.e-sga.org). Figure 1 contains an excerpt from a geological map with superimposed contours of the gravity field (Häning & W. Lange 1996) that covers the SkyTEM resistivity anomaly, which is also marked on the figure. The figure 1 map frame, including the outline of the resistivity anomaly is used throughout this report for the display of other types of data. The geological and gravity data map is a scanned version of GLA, Geologisches Landesamt Sachsen-Anhalt: Gravimetrische Übersichtskarte von Sachsen-Anhalt mit Geologischen Strukturen 1:400.000, 1 mGal equidistance.D (Häning & W. Lange 1996).

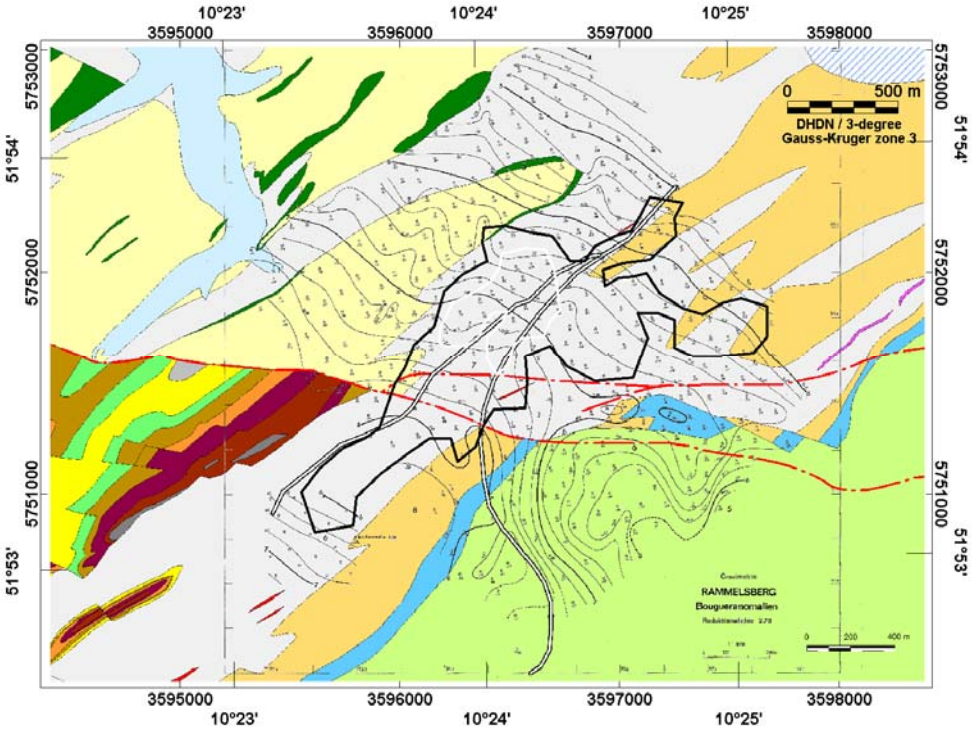

Figure 1. *Geological map of the Gosetal area with superimposed contours of the Bouguer gravity anomaly (gravity data from Plaumann, 1971). The polygons in black and white colours outline the SkyTEM anomaly (outer and inner part of anomaly; see also section 3.2 below). The map frame is used throughout this report for other types of data displays. Similarly, the polygons are superimposed on the succeeding maps for reference.*

3.2 Electromagnetic data

The airborne time-domain survey is described in a report by SkyTEM ApS (2009). Included in the report are modelling results based on one-dimensional multi-layer models. Figure 2 shows the main anomaly observed by the SkyTEM system, and is here presented as the mean resistivity for the depth interval of 140-160 m above sea level. This depth interval corresponds to a depth below terrain of 180-200 m at the centre of the SkyTEM anomaly. The polygons in grey and white colours are used for reference throughout this report, and represent the outer and inner part of the resistivity anomaly respectively.

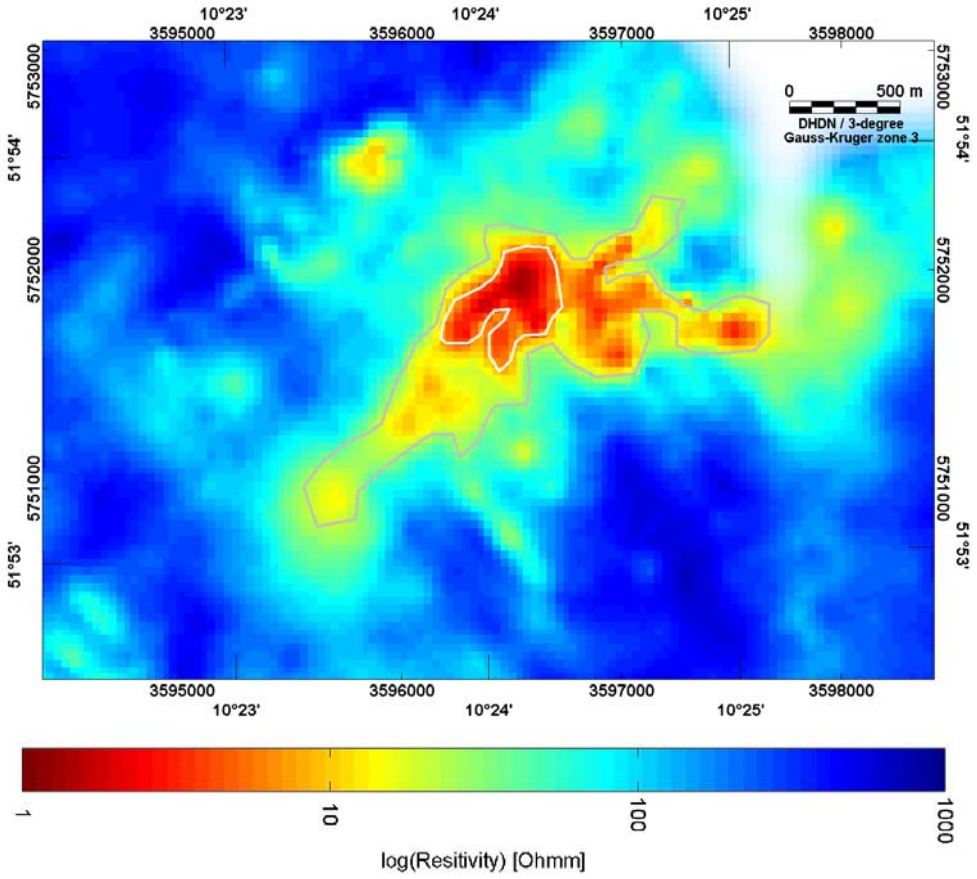

Figure 2. *Map of the SkyTEM anomaly (mean resistivity) at elevation 140-160m. The polygons in grey and white colours are used for reference in other maps and represent the outer and inner part of the resistivity anomaly respectively.*

3.3 Soil gas data

A map based on analysis of soil gas (Figure 3) shows an anomaly co-located with the SkyTEM anomaly.

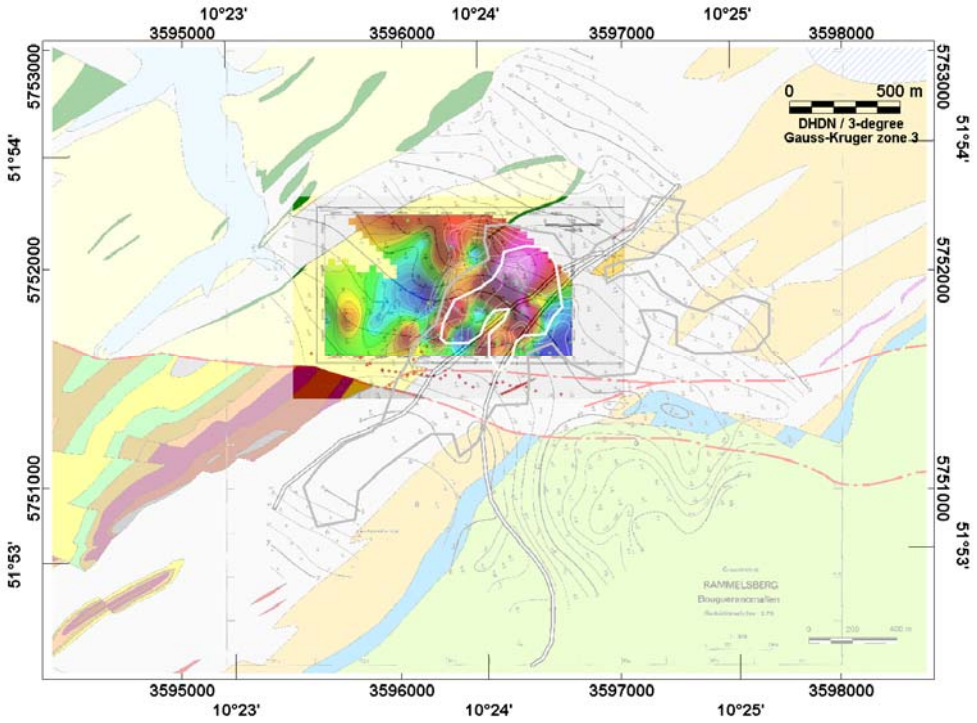

Figure 3. *Soil gas anomaly and geological map. Polygons in grey and white colours outline the outer and inner part of the resistivity anomaly (Figure 2). Data source: Scandinavian Highlands*

3.4 Topography

Two grids with elevation data were provided for this report:

- A grid with lateral resolution of 12.5 m covering the area with gravity data.
- A larger grid with lateral resolution of 50 m encompassing the Gostal area.

Elevation data were furthermore provided by Plaumann (1971) at each gravity station. The two grids were merged with the original Plaumann (1971) elevation data in order to obtain a new digital elevation model that will be used in this report for calculation of Bouguer anomalies.

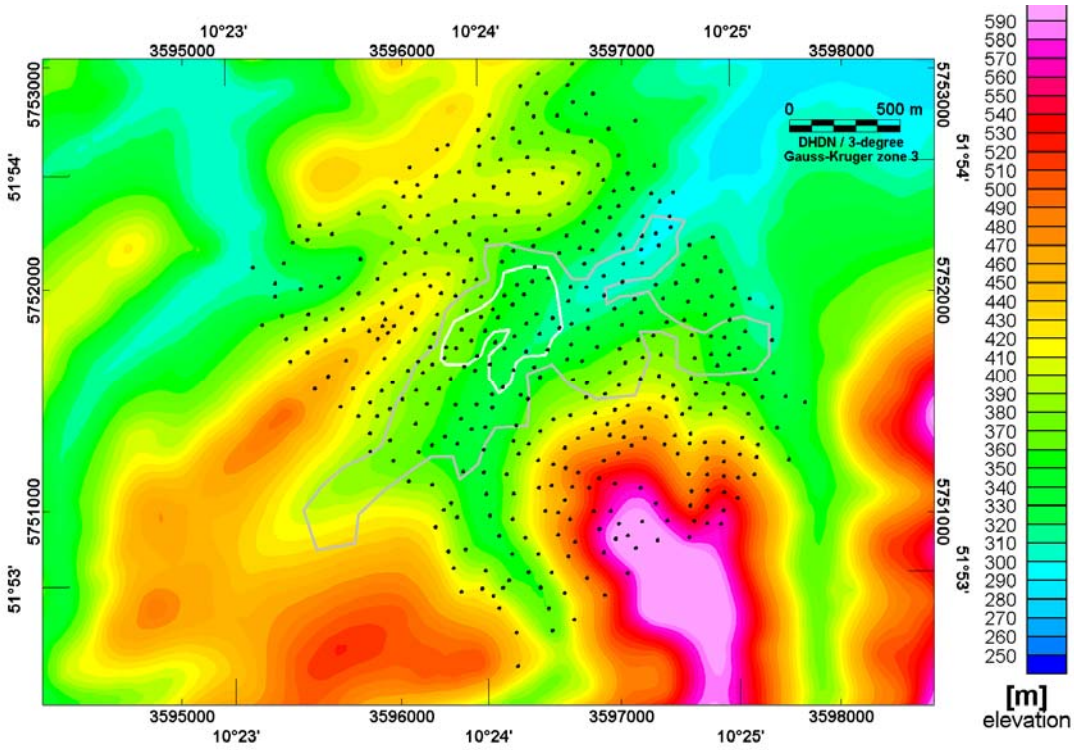

Figure 4. *Topography of the Gosetal area. Black dots mark the location of gravity measurements reported by Plaumann (1971). Polygons in grey and white colours outline the outer and inner part of the resistivity anomaly (Figure 2).*

3.5 Gravity

The gravity data are documented in the report by Plaumann (1971). Plaumann (1971) lists the initial measured values and height information together with two sets of terrain corrections based on replacement densities of 2.60 g/cm^3 and 2.70 g/cm^3 respectively. Two sets of complete Bouguer anomalies corresponding to the two choices of densities are available. The term 'complete Bouguer' is adopted from Blakely (2001) and is defined as the gravity anomaly involving both plate correction (simple Bouguer) and terrain correction. It is unclear, which topography data Plaumann used for terrain corrections, but clearly his topography data were of lower resolution than the data used in the present report (Section 3.4). Plaumann does not mention which model he used to correct for the normal gravity field of the Earth (latitude correction), but a recalculation of the Bouguer values shows that the International Gravity Formula of 1930 has been used. Although the International Gravity Formula of 1930 is superseded by more recent models (1967 and 1980), this report will nevertheless use the 1930 formula since the difference between the models is mainly a constant shift in level of the calculated Bouguer anomalies, and, hence of no significance for the analysis presented in this report. In the following the term Bouguer anomaly is used throughout and refers to the complete Bouguer anomaly (similar to terminology of Plaumann (1971)).

Bouguer anomalies have been calculated for this report using the terrain model described in section 3.4, and using replacement densities of 2.50 g/cm^3 , 2.60 g/cm^3 and 2.70 g/cm^3.

Interpolation of data is performed into grids with grid node distance of 25 m. Figures 5 and 6 shows Bouguer anomaly grids based on the original values provided by Plaumann (1971) for replacement densities of 2.60 g/cm^3 and 2.70 g/cm^3 respectively, and Figures 7 and 8 shows the corresponding grids based on recalculated terrain corrections. Figure 9 and 10 shows the difference between the Bouguer anomalies of Plaumann and the recalculated anomalies (identical to differences in the terrain corrections applied) for replacement densities of 2.60 g/cm^3 and 2.70 g/cm^3 respectively. In general the recalculated values are slightly higher (0.1 mGal mean value) than values provided by Plaumann (1971). The short wavelength deviations in the difference between the original Plaumann Bouguer anomaly data and those calculated here is about ± 0.015 mGal in most cases (Figures 9 and 10). With a mean gravity stations separation of about 100 m, these differences are not significant in relation to the present interpretation. The succeeding displays and discussions on data are based solely on recalculated Bouguer anomaly values.

Figure 11 shows the difference between the Bouguer anomalies based on the two replacement densities (e.g. Figures 7 and 8). This map has an important implication with respect to interpretation of the gravity data. The deviation from the mean with respect to wavelength describes how a wrong choice of replacement density will appear in the Bouguer anomalies. In general the deviations are smooth, and any anomaly shorter than those presented in figure 11 can therefore not be attributed to a wrong choice of density. Anomalies with shorter wavelength must therefore imply (1) insufficient terrain model, (2) gravity measurements errors, (3) data are reflecting true variations in density of the ground or (4) any combination of (1)–(3). The deviations in Figure 11 are discussed further in the section on interpretation.

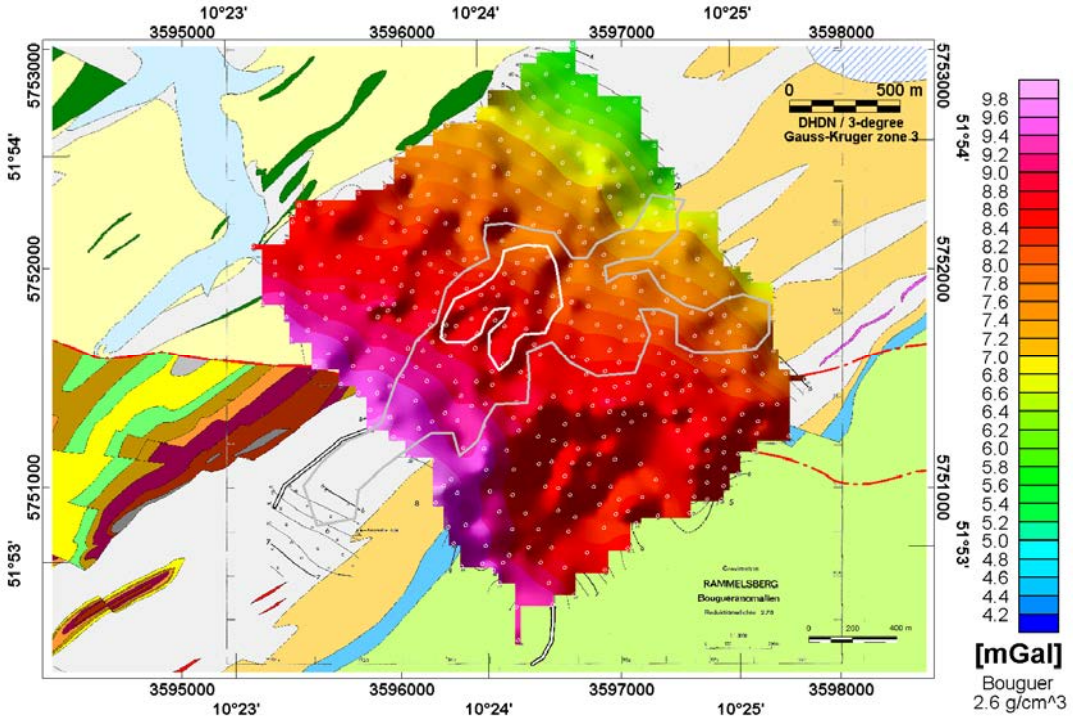

Figure 5. *Grid of Bouguer anomaly with density of 2.6 g/cm^3 used for terrain correction. The grid is based on the calculations provided in Plaumann (1971). Polygons in grey and white colours outline resistivity anomaly (Figure 2). Gravity measuring points are marked in white colour.*

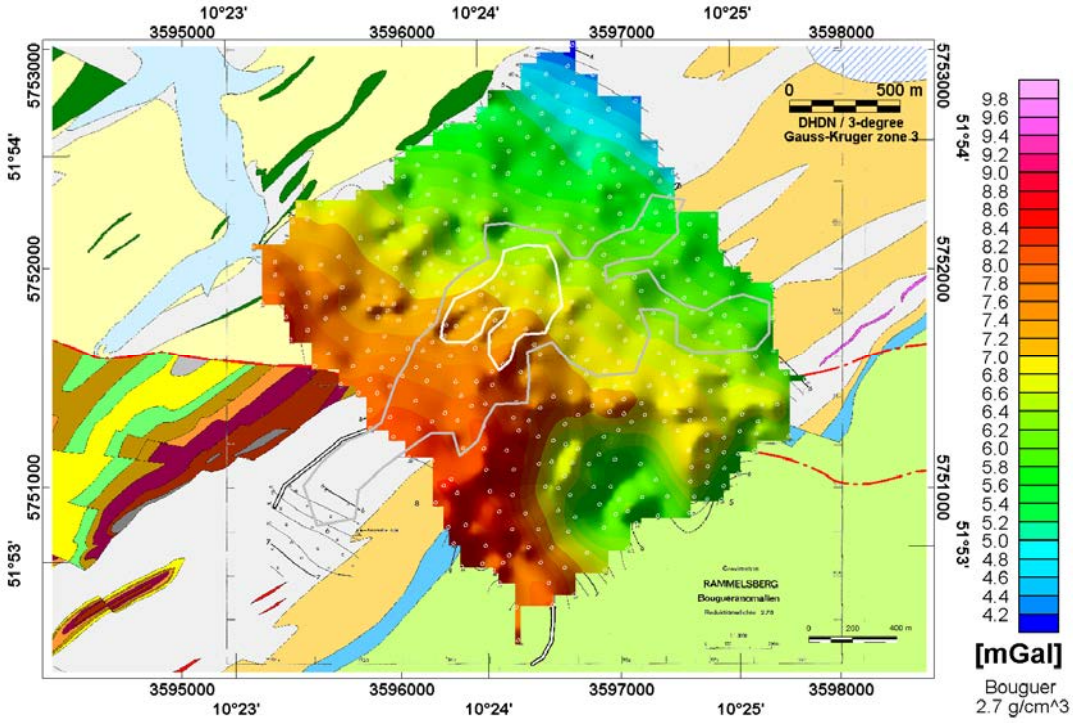

Figure 6. *Grid of Bouguer anomaly with density of 2.7 g/cm^3 used for terrain correction. The grid is based on the calculations provided in Plaumann (1971). Polygons in grey and white colours outline the resistivity anomaly (Figure 2). Gravity measuring points are marked in white colour.*

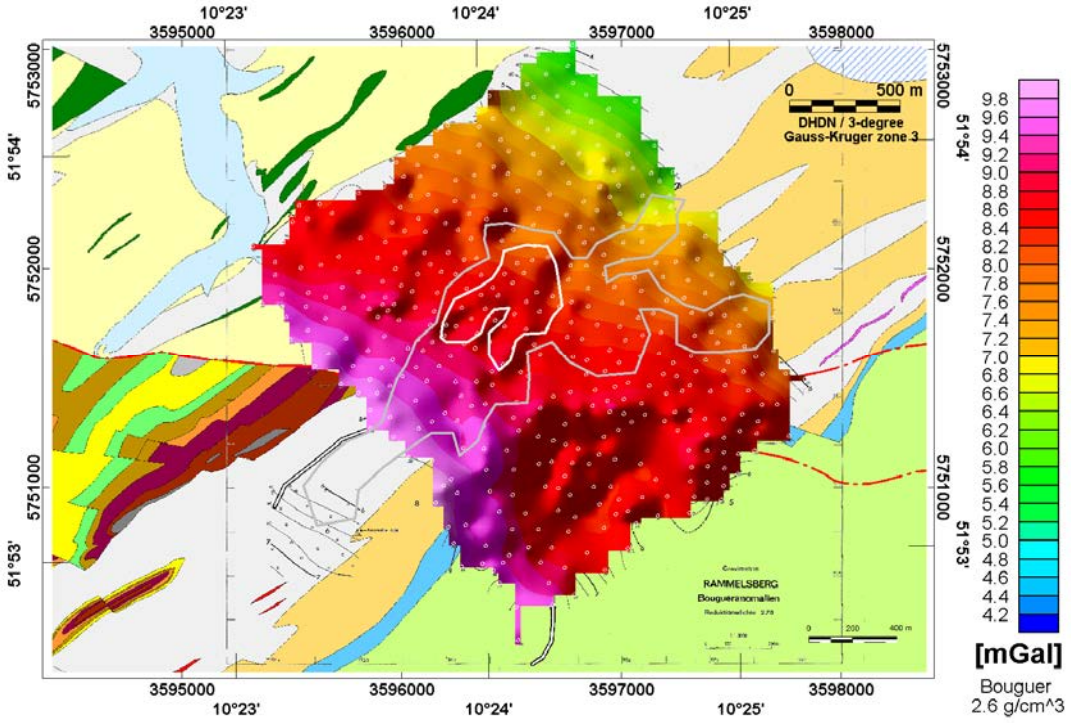

Figure 7. *Grid of Bouguer anomaly with density of 2.6 g/cm^3 used for terrain correction. The grid is derived from recalculated Bouguer values based on the topographic data in Figure 4. Polygons in grey and white colours outline the resistivity anomaly (Figure 2). Gravity measuring points are marked in white colour.*

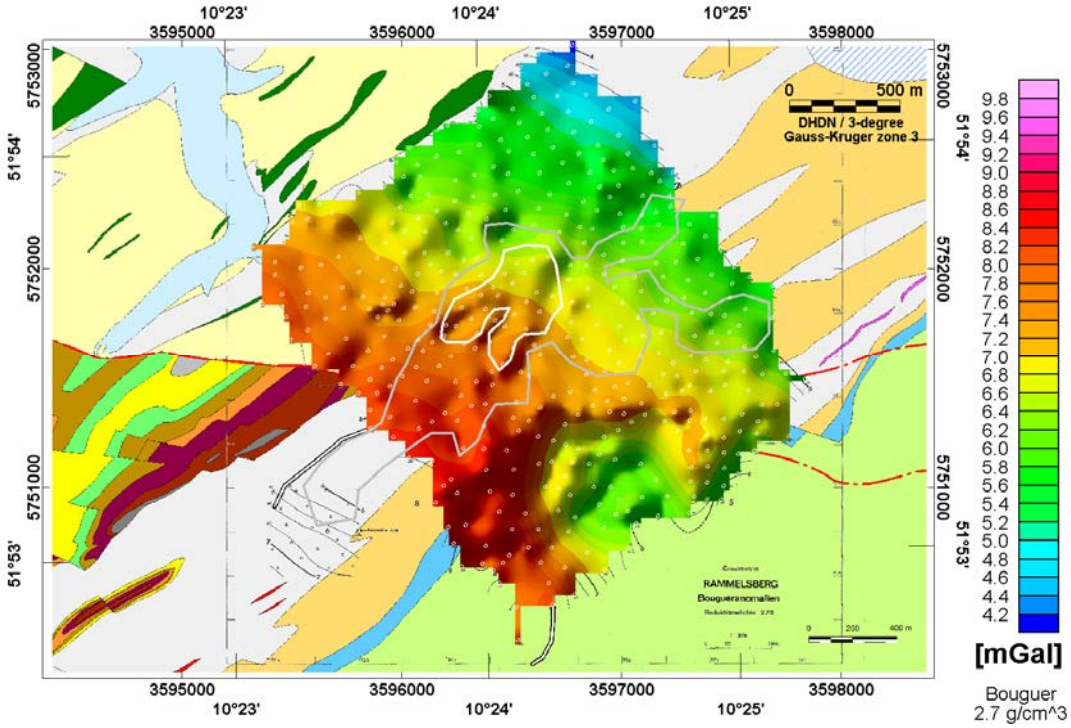

Figure 8. *Grid of Bouguer anomaly with density of 2.7 g/cm^3 used for terrain correction. The grid is derived from recalculated Bouguer values based on the topographic data in Figure 4. Polygons in grey and white colours outline the resistivity anomaly (Figure 2).*

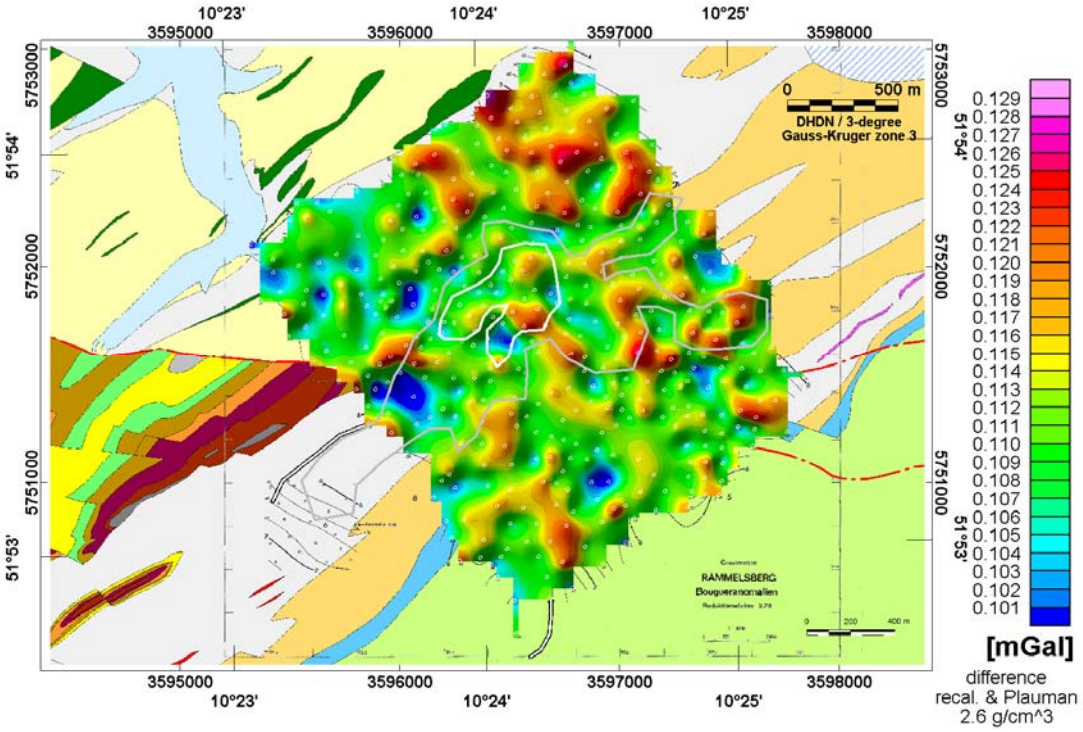

Figure 9. *Differences between recalculated Bouguer values and the values provided by Plaumann (1971). Differences are for a replacement density of 2.6 g/cm^3. Polygons in grey and white colours outline the resistivity anomaly (Figure 2).*

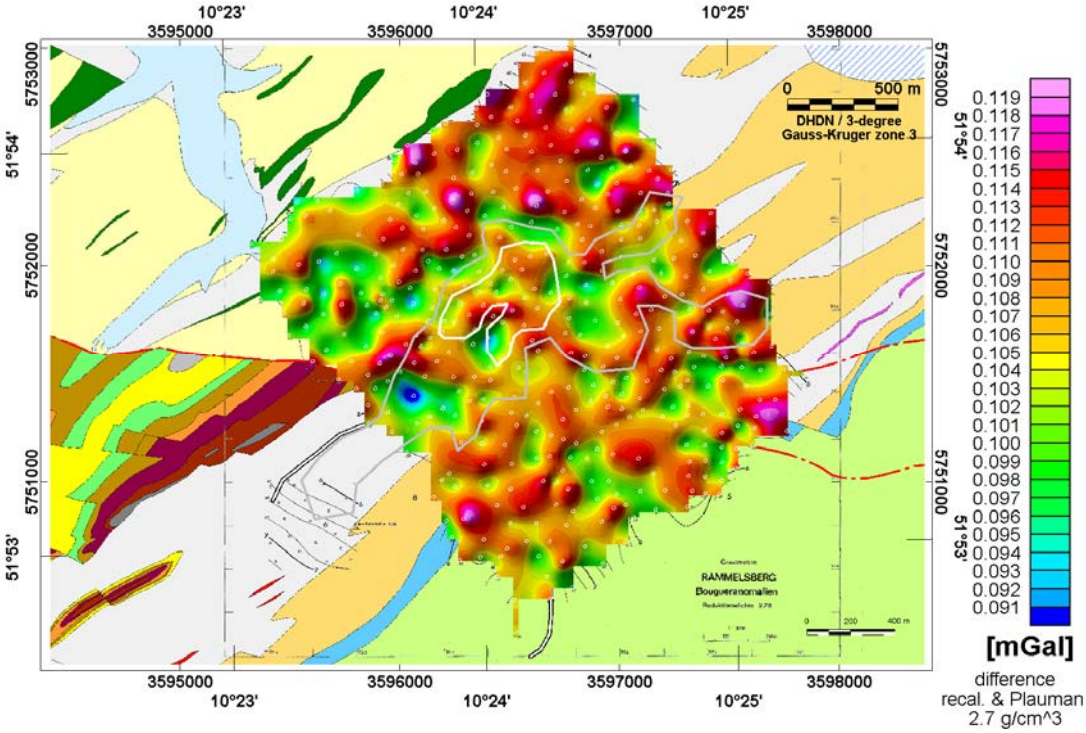

Figure 10. *Differences between recalculated Bouguer values and the values provided by Plaumann (1971). Differences are for a replacement density of 2.7 g/cm^3. Polygons in grey and white colours outline the outer and inner part of the resistivity anomaly (Figure 2).*

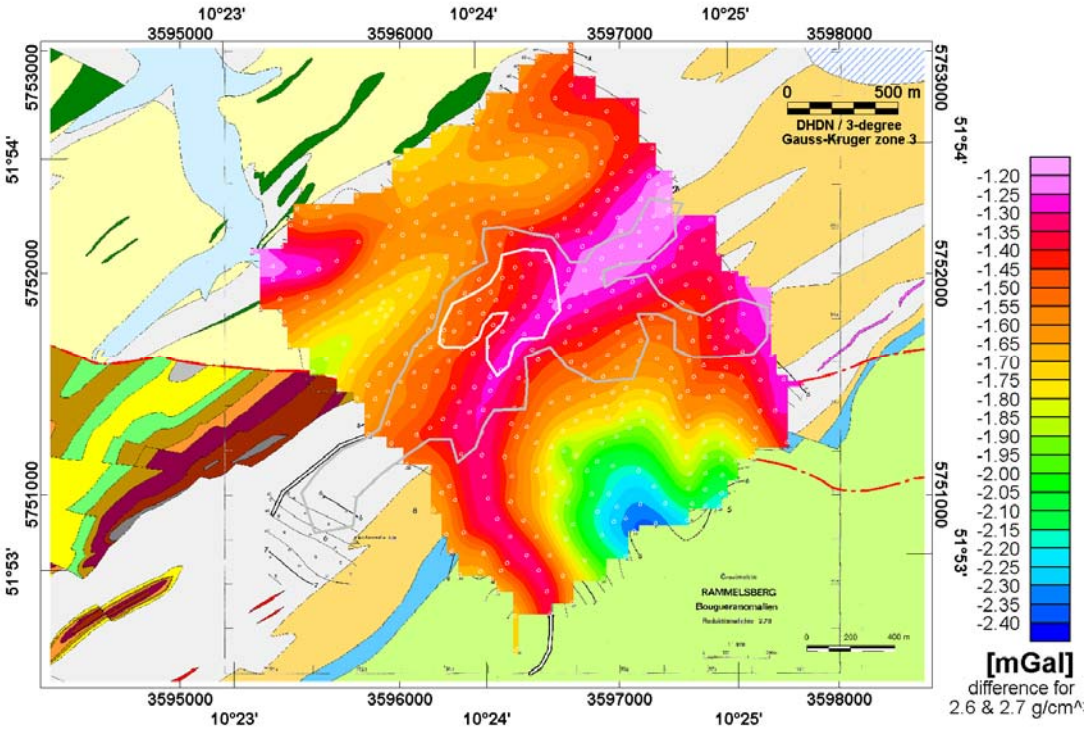

Figure 11. *Differences between Bouguer values for a replacement density of 2.7 g/cm^3 and 2.6 g/cm^3. Bouguer values are based on topographic data in Figure 4. Polygons in grey and white colours outline the outer and inner part of the resistivity anomaly (Figure 2). Gravity measuring points are marked in white colour.*

4. Regional and residual separation

The gravity field in the survey area is characterised by strong horizontal gradients. The following three step procedure has been utilised in order to remove this regional variation in the gravity data. The first step involved spatial averaging of the grid (25 m node separation) with Bouguer gravity data whereby short wavelength anomalies are attenuated. Secondly, this new grid was re-sampled to a 250 m grid node separation. Data from this re-sampled grid were then interpolated with a minimum curvature procedure into a new grid with 25 m node separation, which is used to represent the regional field variations. Regional and corresponding residual grids are displayed in Figures 12 and 13 for a replacement density of 2.6 g/cm^3 and in Figures 14 and 15 for a replacement density of 2.7 g/cm^3. Note that the regional-residual separations are likely to be in error close to the grid boundary.

A comparison between the two grids with residual anomalies and the grid in Figure 11 shows clearly that the residual based on a density of 2.7 g/cm^3 has a significant contribution from topography included along the main valley in the survey area. The residual based on 2.6 g/cm^3 does not show a clear correlation to the grid in Figure 11. A residual grid based on reducing the replacement density to 2.5 g/cm^3 is shown in Figure 16. The shift from a positive anomaly in the 2.7 g/cm^3 grid to negative anomaly in the 2.5 g/cm^3 grid at the southern corner indicates that the 2.6 g/cm^3 choice is a reasonable choice for this particular area, where the most short wavelength topographic effect is seen.

Of particular interest for the interpretation is that the short wavelength residual gravity anomaly located within the main resistivity anomaly is found in all maps (marked A1 in Figure 16). The conclusion is that this anomaly is not caused by a wrong choice of density in the terrain correction. Other anomalies of interest are marked A2 and A3. Anomaly A2 is located within an area of rough terrain. The terrain correction is therefore subjected to possible errors at this location.

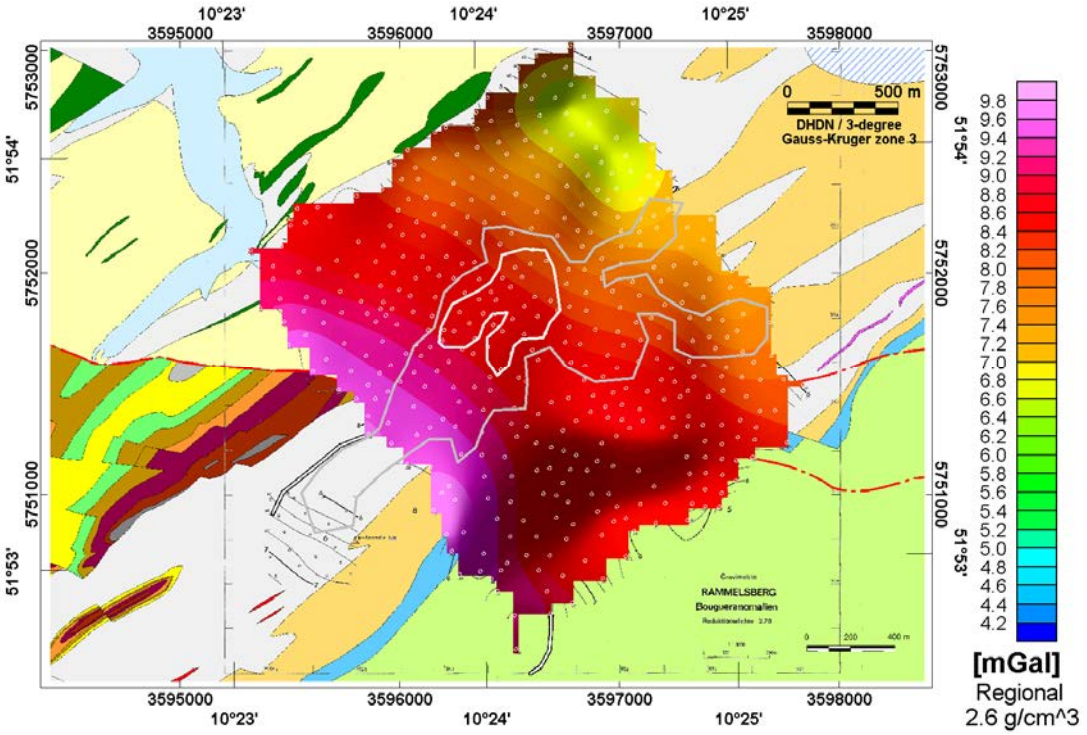

Figure 12. *Grid of regional Bouguer anomalies used for calculation of residual anomalies in Figure 13. Values are for a replacement density of 2.6 g/cm3. Polygons in grey and white colours outline the resistivity anomaly (Figure 2). Gravity measuring points are marked in white colour.*

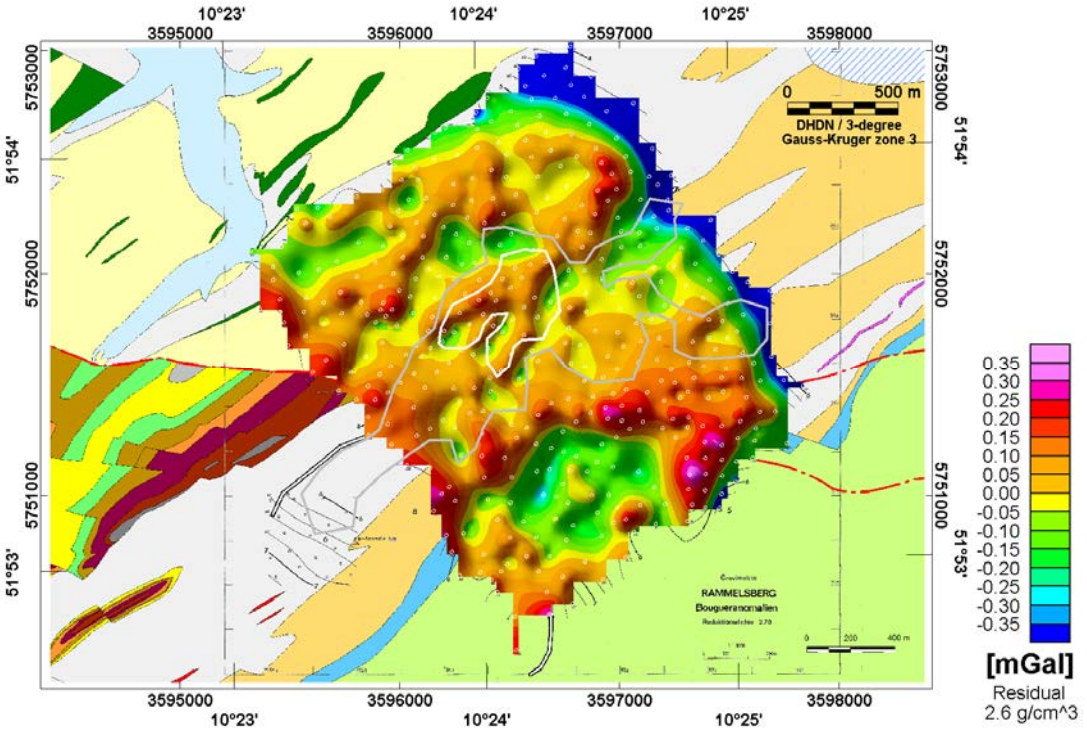

Figure 13. *Grid of residual Bouguer anomalies used for calculation of residual anomalies in Figure 12. Values are for a replacement density of 2.6 g/cm^3. Polygons in grey and white colours outline the resistivity anomaly (Figure 2). Gravity measuring points are marked in white colour.*

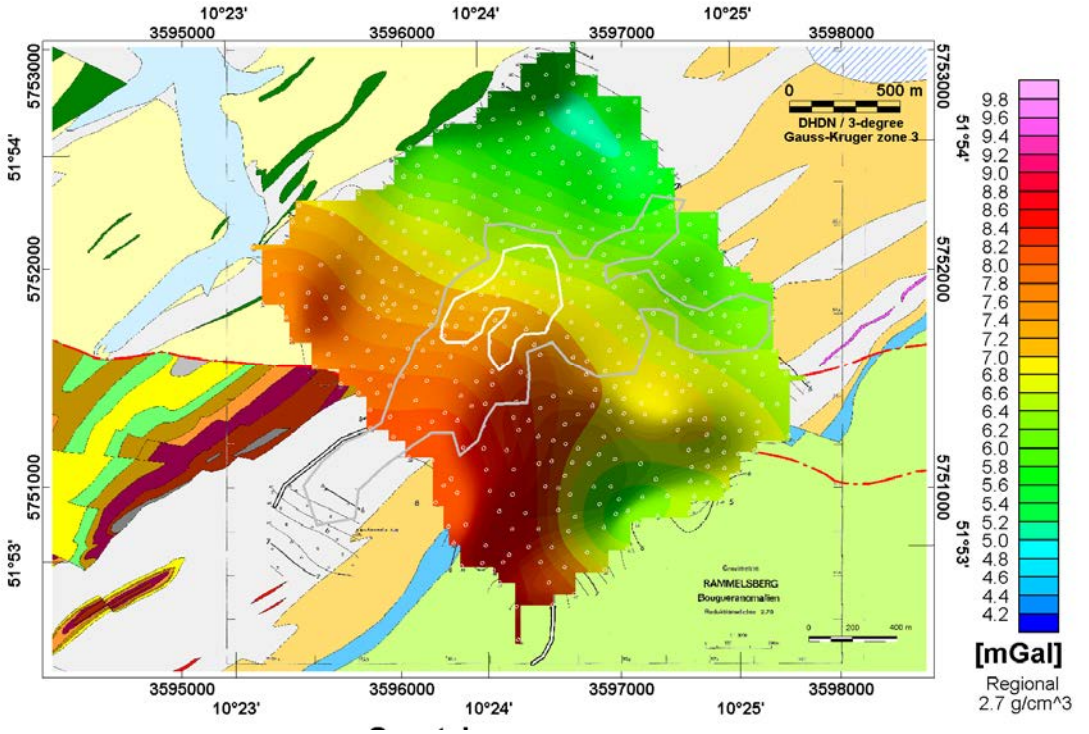

Figure 14. *Grid of regional Bouguer anomalies used for calculation of residual anomalies in Figure 15. Values are for a replacement density of 2.7 g/cm^3. Polygons in grey and white colours outline the resistivity anomaly (Figure 2). Gravity measuring points are marked in white colour.*

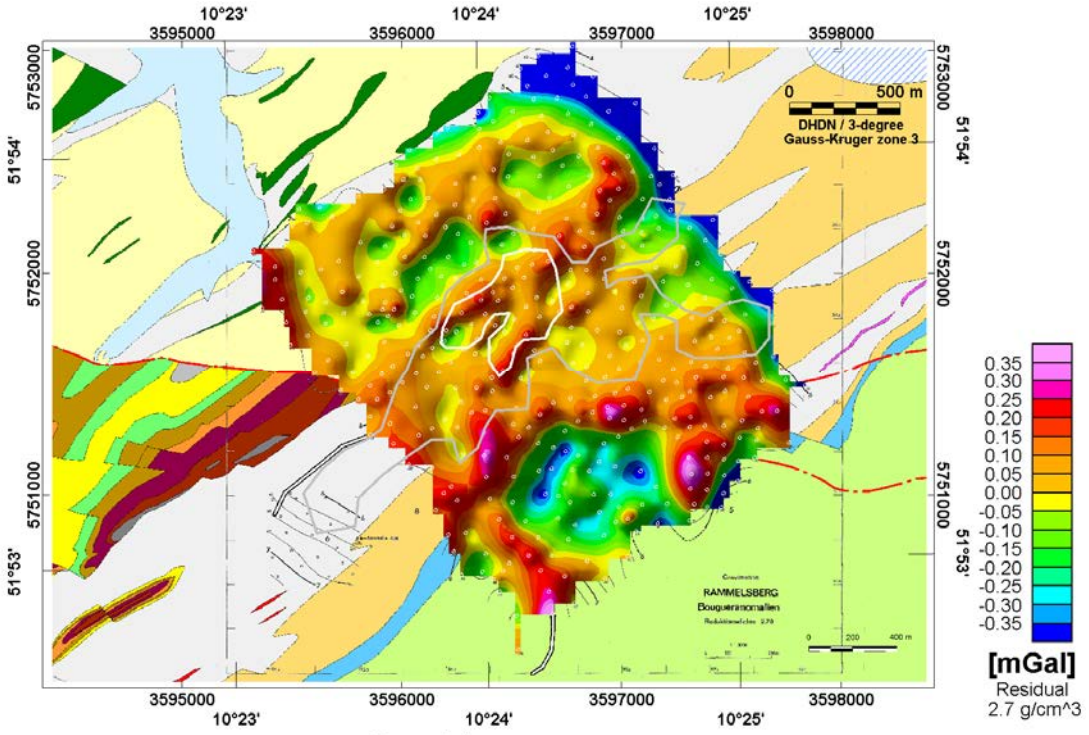

Figure 15. *Grid of residual Bouguer anomalies used for calculation of residual anomalies in Figure 14. Values are for a replacement density of 2.7 g/cm^3. Polygons in grey and white colours outline the resistivity anomaly. Gravity measuring points are marked in white colour.*

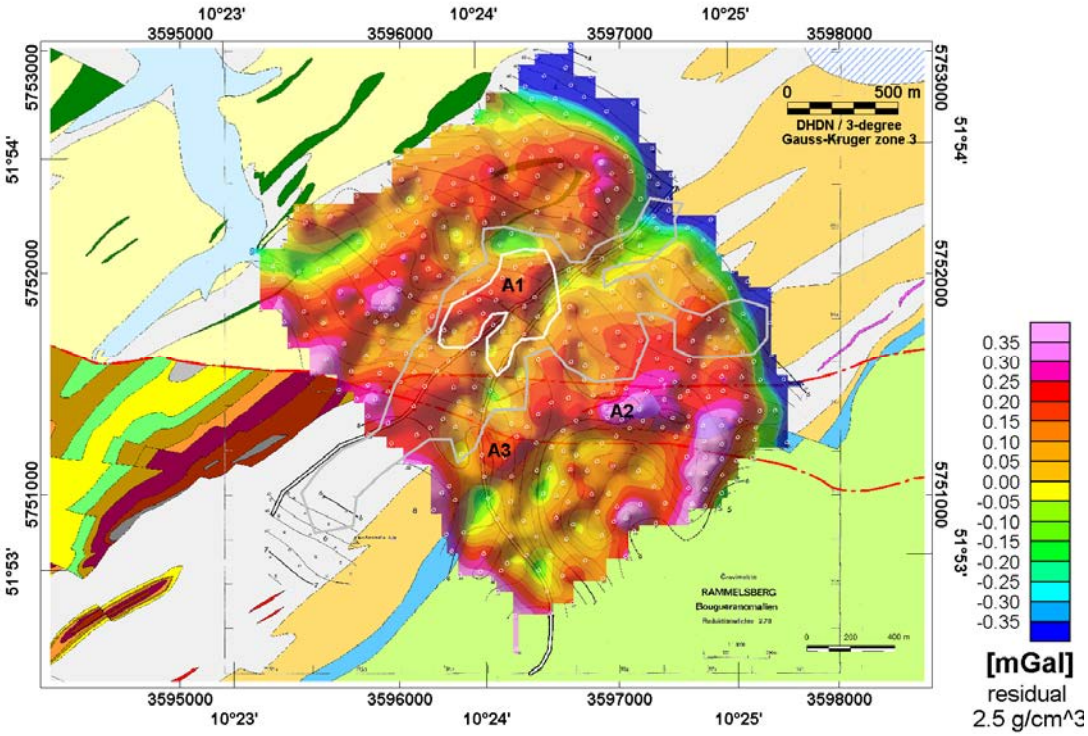

Figure 16. *Grid of residual Bouguer anomalies used for calculation of residual anomalies in Figure 14. Values are for a replacement density of 2.5 g/cm^3. Polygons in grey and white colours outline the resistivity anomaly (Figure 2). Gravity measuring points are marked in white colour. The image of the gravity grid is made transparent in order to view geological map in the background.*

5. Interpretation of gravity data

The gravity anomaly A1 co-located with the resistivity anomaly is clearly of importance in a search for mineralisations. Other areas of interest are along the exposure of marble further south (A2 & A3 in Figure 16), but they are not associated with resistivity anomalies.

In order to guide the interpretation of the gravity data, a catalogue of gravity responses has been produced (See Appendix). The catalogue includes responses from tabular bodies with varying geometry. The density contrast used in the calculations is chosen to 1 g/cm^3 which allow a simple scaling if other values are considered. The tabular bodies are described by the following parameters (values in parenthesis denote ranges in values used):

- Thickness, T [5 m; 55 m]
- Depth to top, z [50 m; 550 m]
- Extent vertically measured from z, E [50 m; 550 m]
- Length along strike, L [100 m; 600 m] (strike orientation is north-south)
- Dip angle, D [7.5 degree; 90 degree]

The responses are shown in a number of Figures in the Appendix. Each row corresponds to 11 different values of one selected parameter and fixed values for the remaining parameters. The step in value is linear with minimum values towards left and maximum values towards right. With the exception of rows 5 to 7, the thickness is either 10 m (Figures A1-A4) or 20 m (Figures A5-A8). For rows 5 to 7, the thickness values vary from 5 to 55 m. The responses are shown in a one-colour presentation such that responses are only displayed if they exceed a chosen threshold value. Threshold values of 0.025, 0.05, 0.10 and 0.2 mGal are used.

Plaumann (1971) evaluates the uncertainty of the calculated Bouguer values to be of the order of ±0.05 to ±0.1 mGal. Inspection of the model responses in the Appendix reveals that these are above the detection limit for a large number of tabular bodies used. However, it is also clear that the gravity response corresponding to a mineralisation with thickness 10-20 m is likely not going to be very strong (see Figures A9 and A10) in comparison to the data uncertainties. Increasing the density contrast above 1 g/cm^3 will obviously improve the possibility to obtain a measurable response.

Three sub-parallel profiles across anomaly A1 have been extracted for modelling with a tabular structure. The use of a tabular body as principal model in the modelling is obvious a simplification considering the actual shape of both the gravity and SkyTEM resistivity anomaly. Nevertheless, the model calculation provides some insight with respect to possible causative structures. In order to account for some long wavelength anomalies that are not removed in the regional-residual separation, a level shift is included in the modelling. By doing this negative values are matched even though the anomaly is modelled by a tabular body with a positive density contrast.

The results of this modelling are displayed in Figures 17-22. Data from each profile were subjected to an automatic data inversion scheme. For each profile an inversion was done with all parameters free and another inversion was done with the dip angle fixed to a value of 60 degrees towards SE. All models are able to reproduce the data at an acceptable level, when considering the uncertainties (including interpolation inaccuracies and uncertainties involved in terrain correction). The small difference in data fit for fixed and free values of the dip angle in the inversion imply that the data do not constrain this parameter. For all six models, densities above 3.5 are obtained.

Interpretation of gravity data is inherently ambiguous and much care must be made with respect to possible conclusions from the presented data and modelling. A perfect match in response is also possible by simple variations in surface density. The main conclusion from the modelling is that the gravity data are consistent with, and certainly do not exclude the presence of an ore body below the SkyTEM anomaly. It is furthermore concluded that the observed gravity anomaly is unlikely to be caused by erroneous correction for topographic effects.

In order to add more confidence to the interpretation of the gravity data, density information on both host rocks and potential mineralisation are required. Improvements are also possible by denser gravity station spacing.

The choice of gravity station separation for new gravity measurements should be based on an evaluation of the obtained data on site during the survey campaign. An initial sampling of 10 m along profiles will provide important insight with respect to wavelength content and half-width of the gravity anomalies. The station separation may be increased slightly if the gravity field is varying smoothly. However, it is important to keep in mind that the thickness of a mineralised zone is of the order of 10 m and a dense sampling is therefore required.

The half-width of gravity anomaly is highly dependent on the depth to the anomalous zones. Variations in surface density may therefore have a significant influence on the observed gravity field and lead to erroneous conclusions on possible mineralisations at depth. In order to evaluate and exclude this possibility, surface samples should be obtained for density measurements in the surveyed area.

Profiles across anomaly A1 is proposed. A choice of 50 m separation between profile lines may be used initially. The choice should be evaluated during the survey campaign in order to optimize the survey. The profile length should be sufficiently long to define the anomaly half-width properly; e.g. a clear minimum should be measured on both side of the anomaly.

Anomalies A2 and A3 should be covered by stations arranged in grids. The node distance should be decided on site after some initial profiling with dense station (10-20m) separation.

Another possibility of adding more confidence to the conclusions is further data integration. In particular the SkyTEM data should be re-evaluated together with existing information from boreholes.

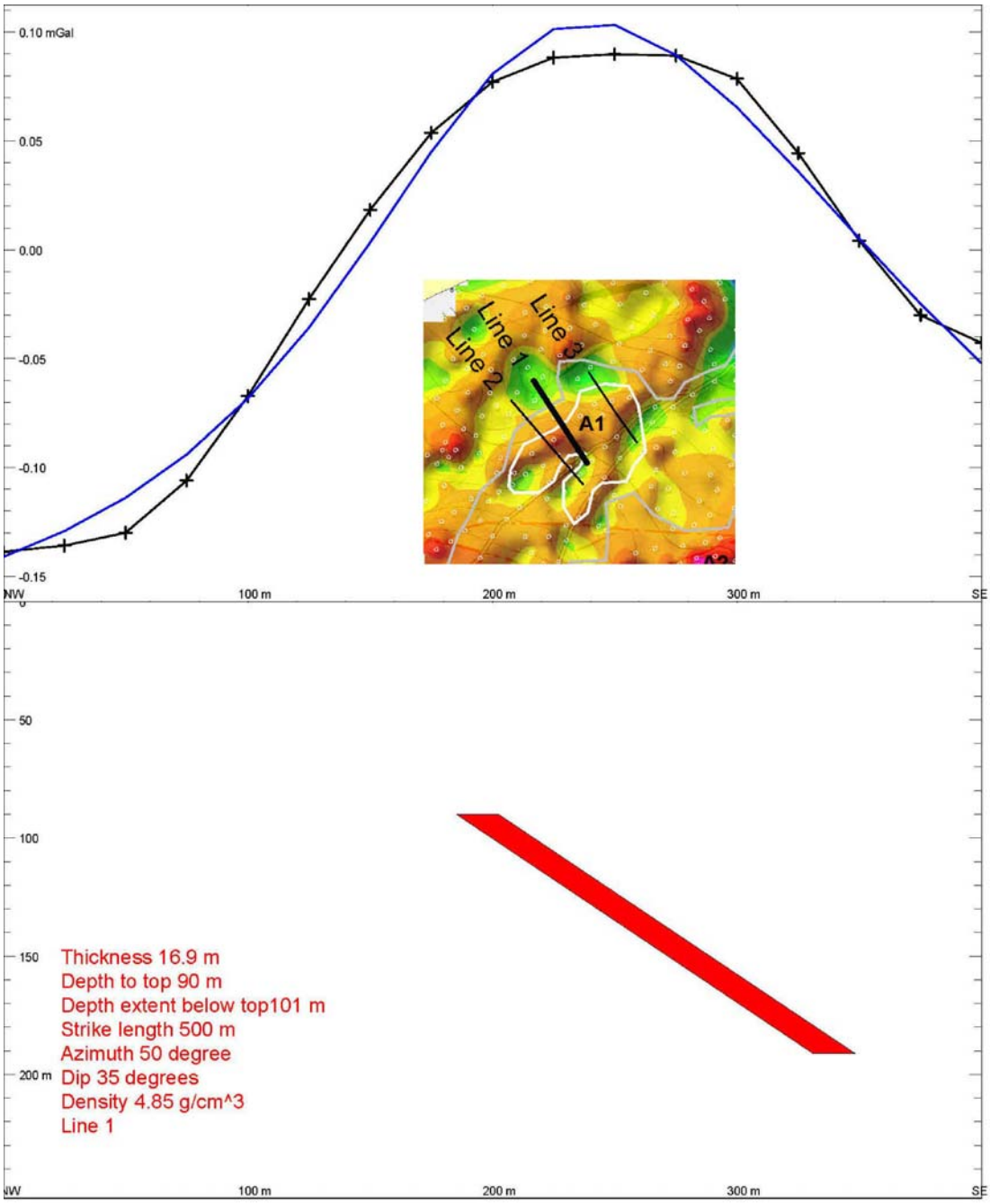

Figure 17. *Results of modelling of anomaly A1 extracted along profile 1 from the residual gravity anomaly based on a replacement density of 2.67 g/cm3. The curve in black colour is the residual anomaly and the curve in blue colour is the model response. A constant level shift is applied to the model response data in order match the data with negative sign towards north-east.*

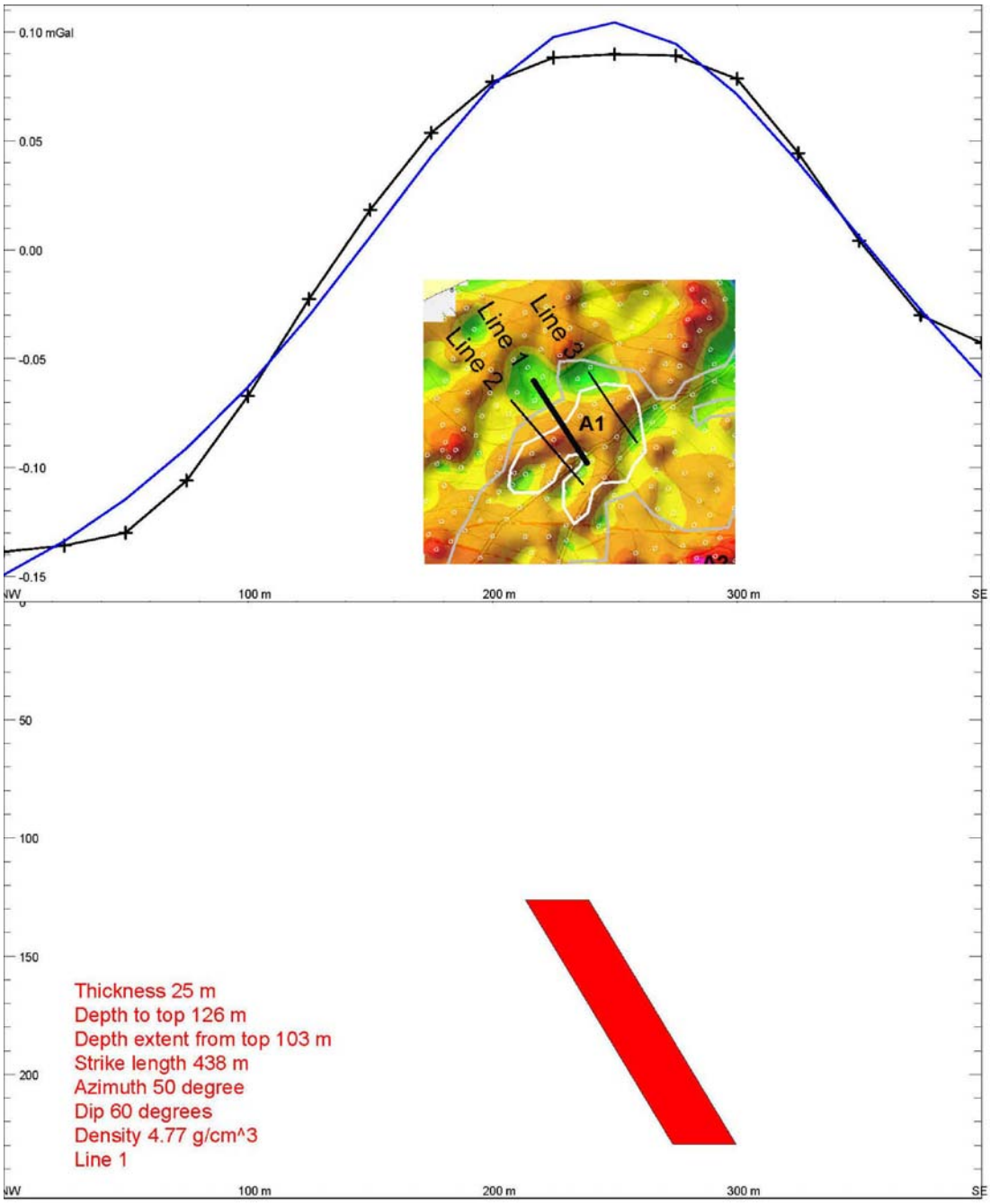

Figure 18. *Results of modelling of anomaly A1 extracted along profile 1 from the residual gravity anomaly based on a replacement density of 2.67 g/cm3. The dip angle was fixed at 60 degrees towards SE. The curve in black colour is the residual anomaly and the curve in blue colour is the model response. A constant level shift is applied to the model response data in order match the data with negative sign towards north-east.*

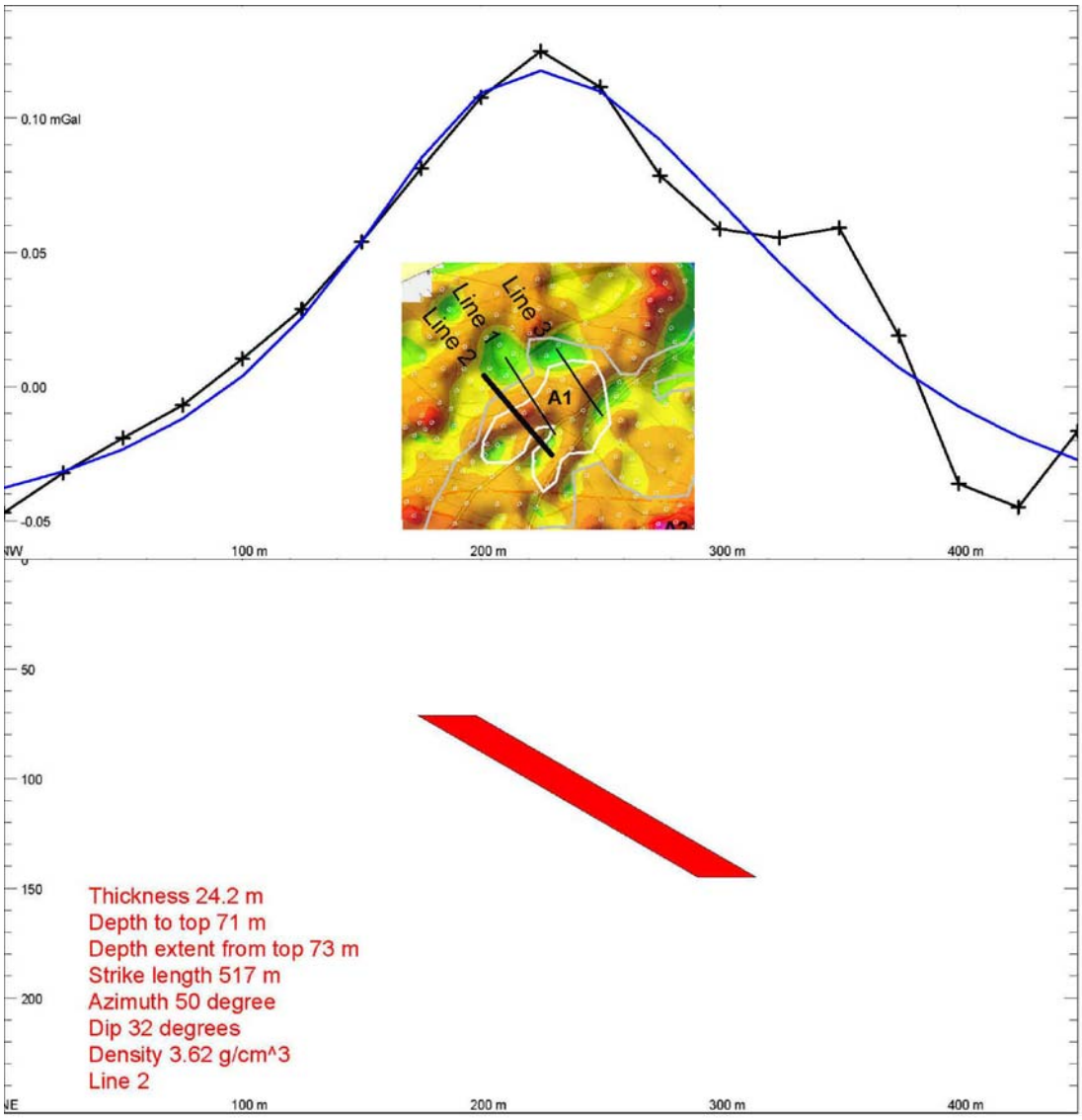

Figure 19. *Results of modelling of anomaly A1 extracted along profile 2 from the residual gravity anomaly based on a replacement density of 2.67 g/cm3. The curve in black colour is the residual anomaly and the curve in blue colour is the model response. A constant level shift is applied to the model response data in order match the data with negative sign towards north-east.*

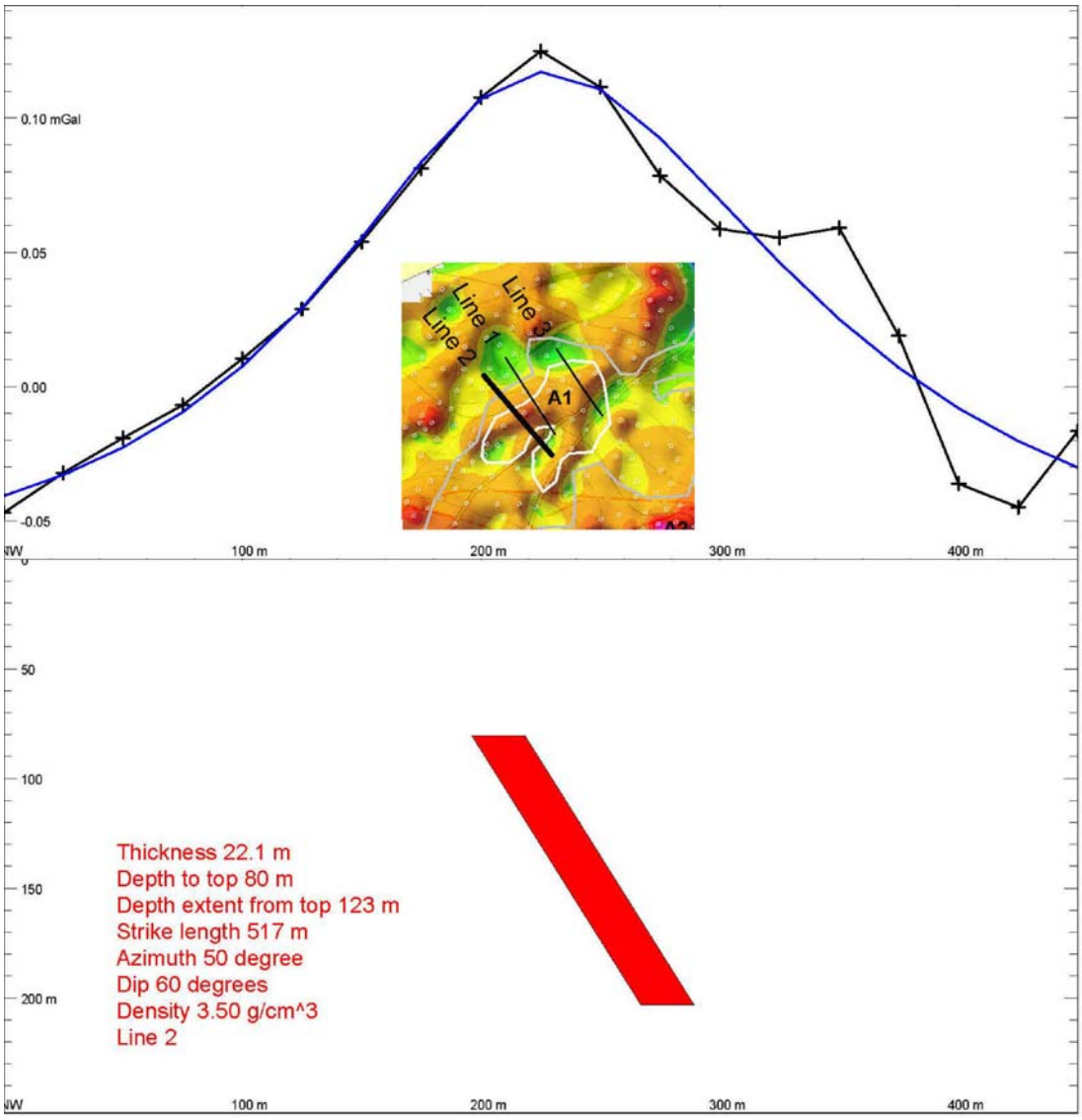

Figure 20. *Results of modelling of anomaly A1 extracted along profile 2 from the residual gravity anomaly based on a replacement density of 2.67 g/cm3. The dip angle was fixed at 60 degrees towards SE. The curve in black colour is the residual anomaly and the curve in blue colour is the model response. A constant level shift is applied to the model response data in order match the data with negative sign towards north-east.*

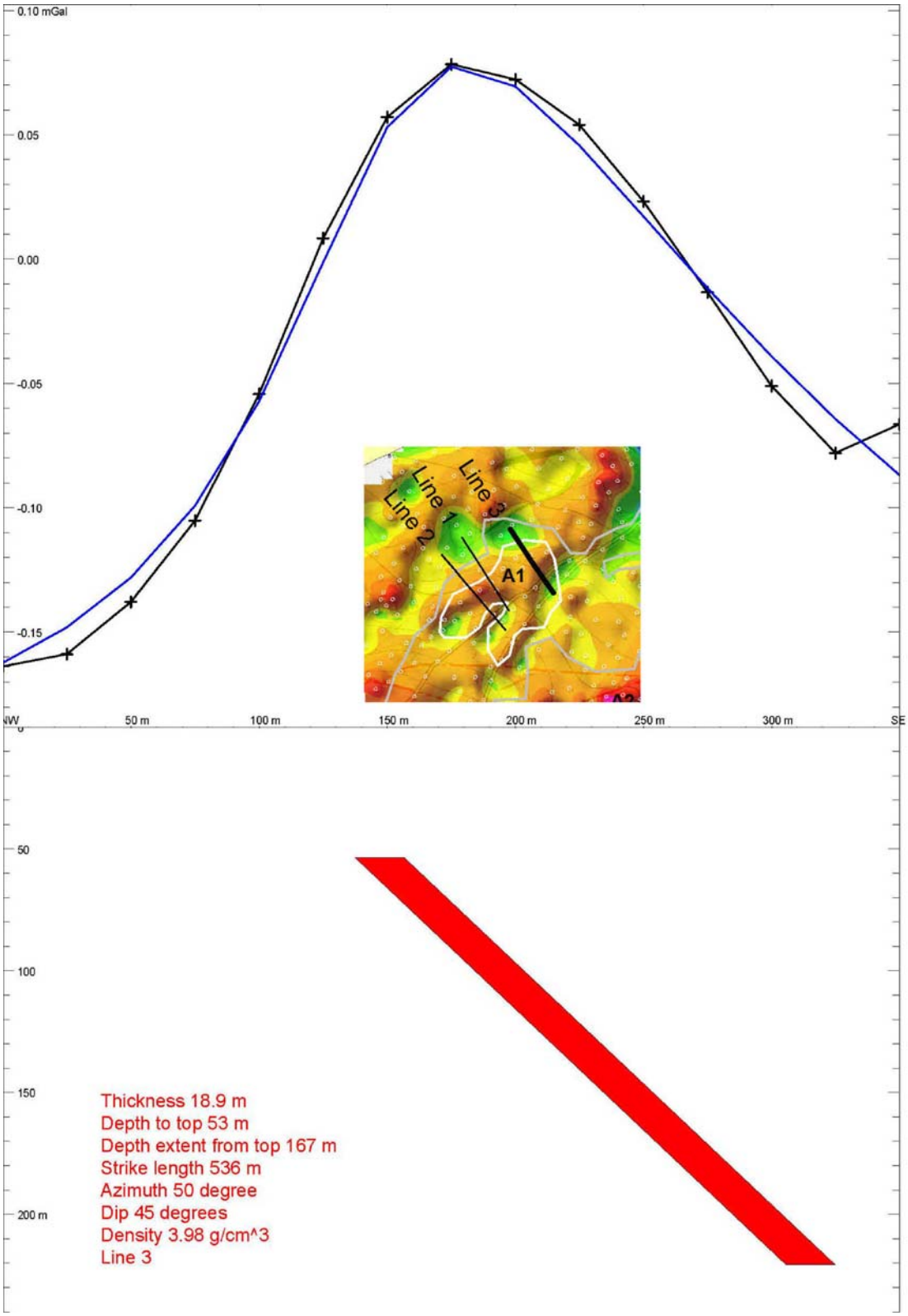

Figure 21. *Results of modelling of anomaly A1 extracted along profile3 from the residual gravity anomaly based on a replacement density of 2.67 g/cm3. The curve in black colour is the residual anomaly and the curve in blue colour is the model response. A constant level shift is applied to the model response data in order match the data with negative sign towards north-east.*

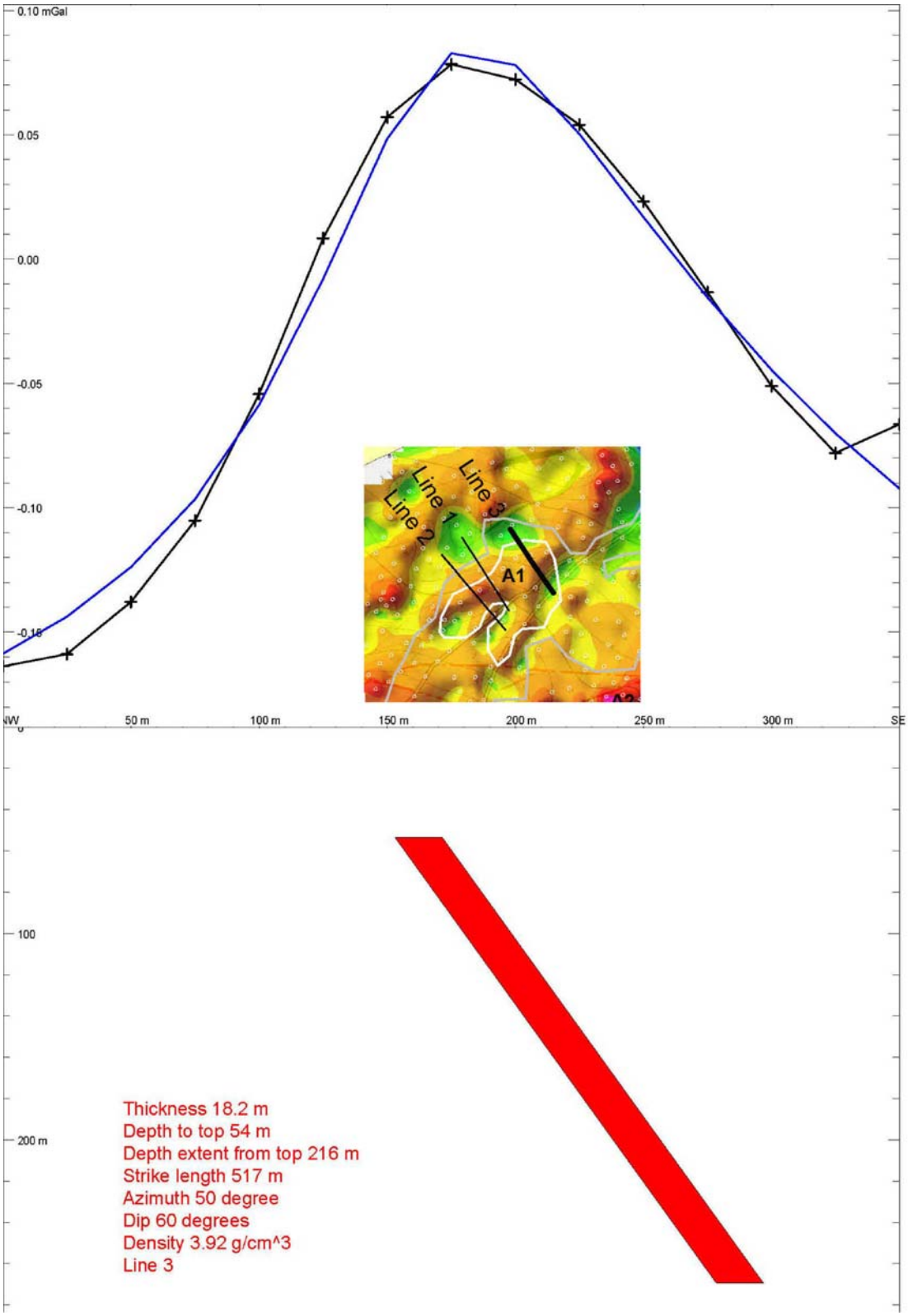

Figure 22. *Results of modelling of anomaly A1 extracted along profile3 from the residual gravity anomaly based on a replacement density of 2.67 g/cm3. The dip angle was fixed at 60 degrees towards SE. The curve in black colour is the residual anomaly and the curve in blue colour is the model response. A constant level shift is applied to the model response data in order match the data with negative sign towards north-east.*

6. References

Blakely, R.J. 2001: Potential Theory in Gravity and Magnetic Applications. Cambridge University Press. ISBN 0-521-57547-8.

Brink, H-J., 2011: The crustal structure around the Harz Mountains (Germany): review and analysis. Z.dt.Ges.Geowiss., 162/3, p. 235-250, 13 figs.

Häning, D & Lange, W. 1996: Scan of GLA, Geologisches Landesamt Sachsen-Anhalt: Gravimetrische Übersichtskarte von Sachsen-Anhalt mit Geologischen Strukturen 1:400.000, 1 mGal equidistance. ISBN 3-929951-14-2, Geocoded by TSL, Checked by HS 26/02-2009.

Plaumann, S., 1971: Bericht über Schweremessungen am Ramelsberg bei Goslar. Niedersächsisches Landesamt für Bodenforschung, Hannover. Archiv 0005897.

SkyTEM ApS, 2009: SkyTEM Survey Harz, Germany, Data report, January 2009, SkyTEM ApS, Data Report – Harz.

7. Appendix – Catalogue of model responses

Gravity responses from tabular bodies are displayed. The tabular bodies are separated in space such that an anomaly from one tabular body has insignificant influence at the location of the anomaly for other tabular bodies. Locations of tabular bodies are in 13 rows and 11 columns. Locations are marked by circles having radius of 1000 m from the centre of the body.

Each row corresponds to 11 different values of one selected parameter and fixed values for the remaining parameters. The density contrast used in the calculations is chosen to 1 g/cm^3 which allow a simple scaling if other values are considered. The tabular bodies are described by the following parameters (values in parenthesis denote ranges in values used):

- Thickness, T [5 m; 55 m]
- Depth to top, z [50 m; 550 m]
- Extent vertically measured from z, E [50 m; 550 m]
- Length along strike, L [100 m; 600 m] (strike orientation is north-south)
- Dip angle, D [7.5 degree; 90 degree]

The step in value is linear with minimum values towards left and maximum values towards right. With the exception of rows 5 to 7, the thickness is either 10 m (Figures A1-A4) or 20 m (Figures A5-A8). For rows 5 to 7, the thickness values vary from 5 to 55 m. The responses are shown in a one-colour presentation such that responses are only displayed if they exceed a chosen threshold value. Threshold values of 0.025, 0.05, 0.10 and 0.2 mGal are used.

Figures A9 and A10 displays the responses using a full colour scale for the two sets (10 m and 20 m) of tabular bodies.

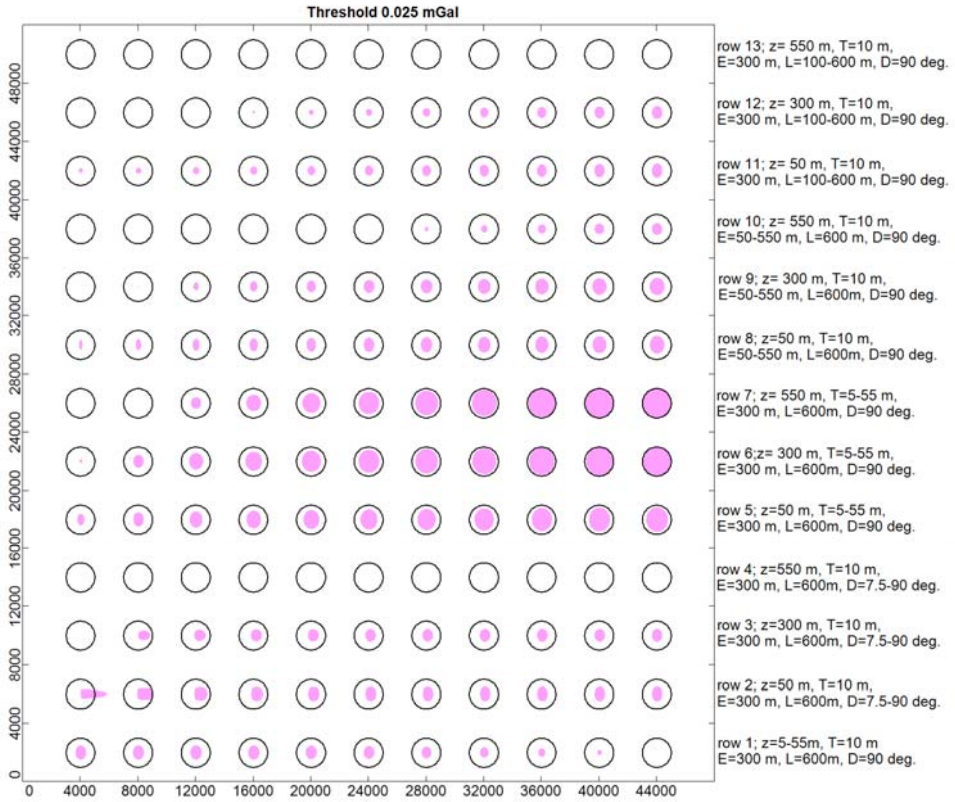

Figure A1. *Thickness 10 m (except rows 5-7) and threshold of 0.025 mGal.*

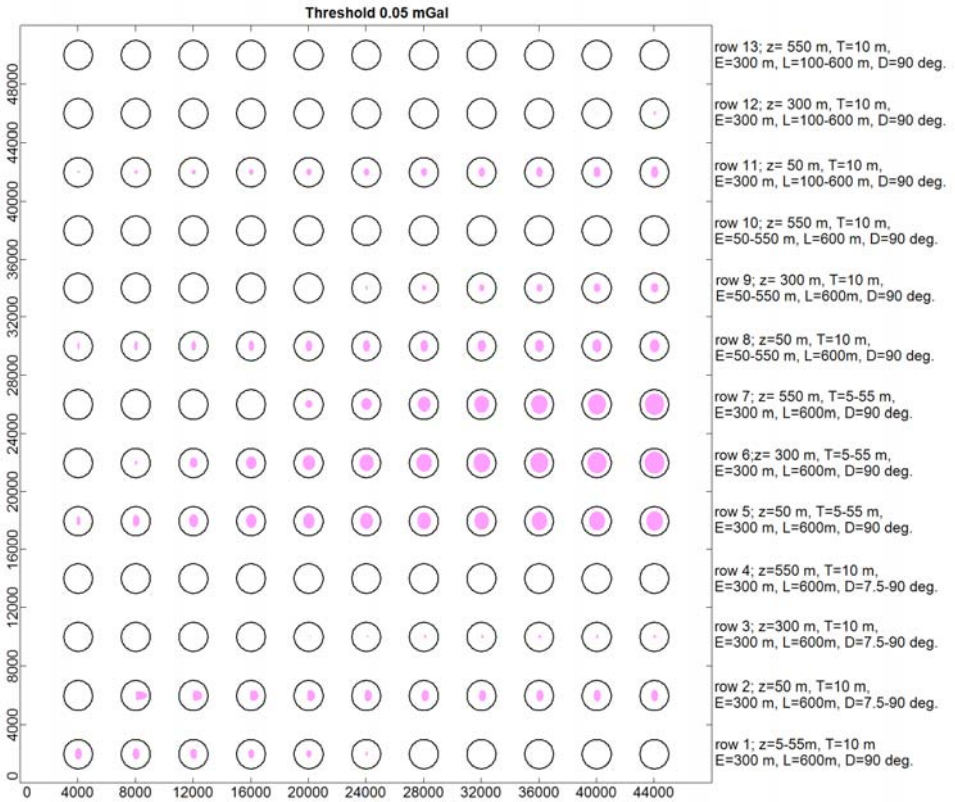

Figure A2. *Thickness 10 m (except rows 5-7) and threshold of 0.05 mGal.*

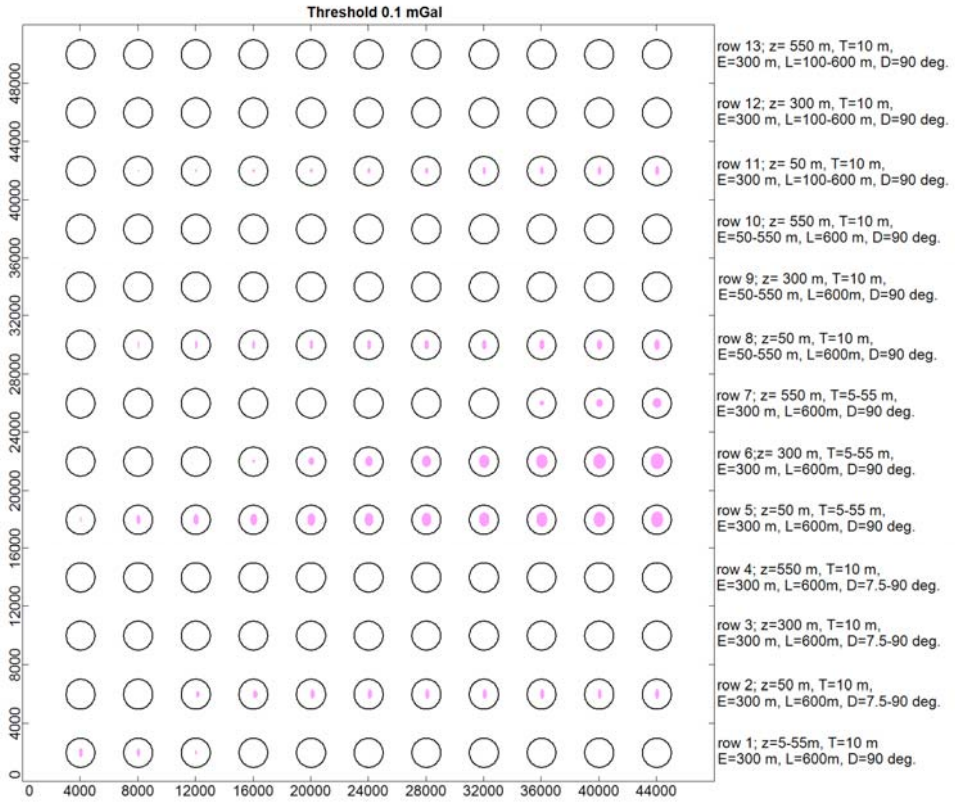

Figure 23. *Thickness 10 m (except rows 5-7) and threshold of 0.10 mGal.*

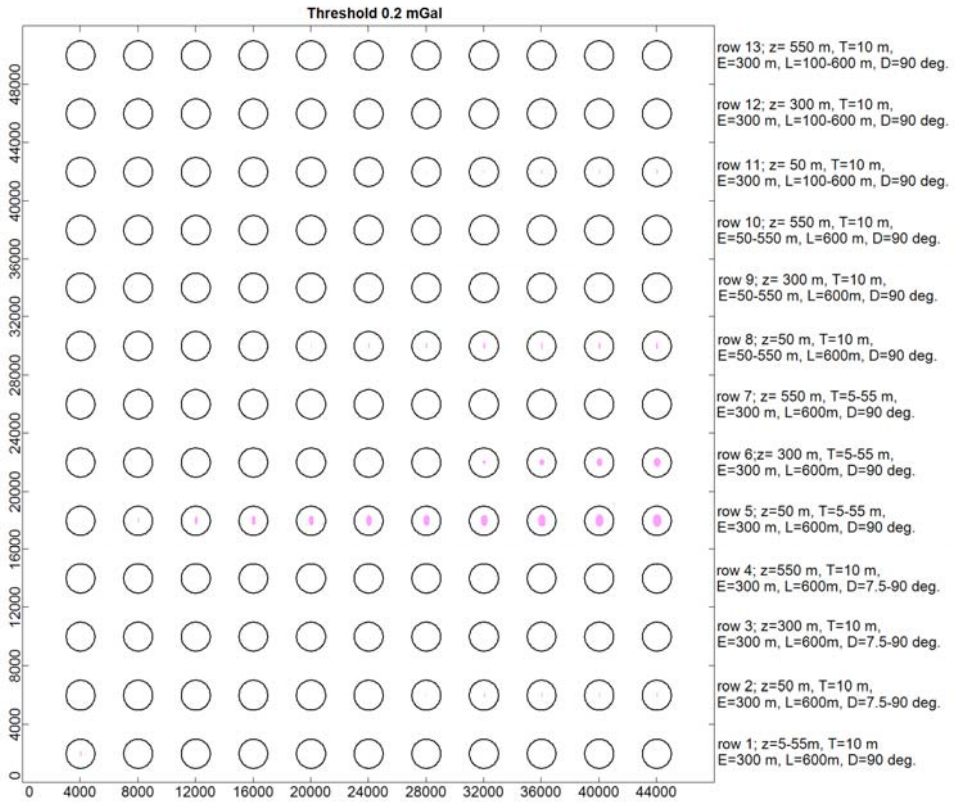

Figure A4. *Thickness 10 m (except rows 5-7) and threshold of 0.2 mGal.*

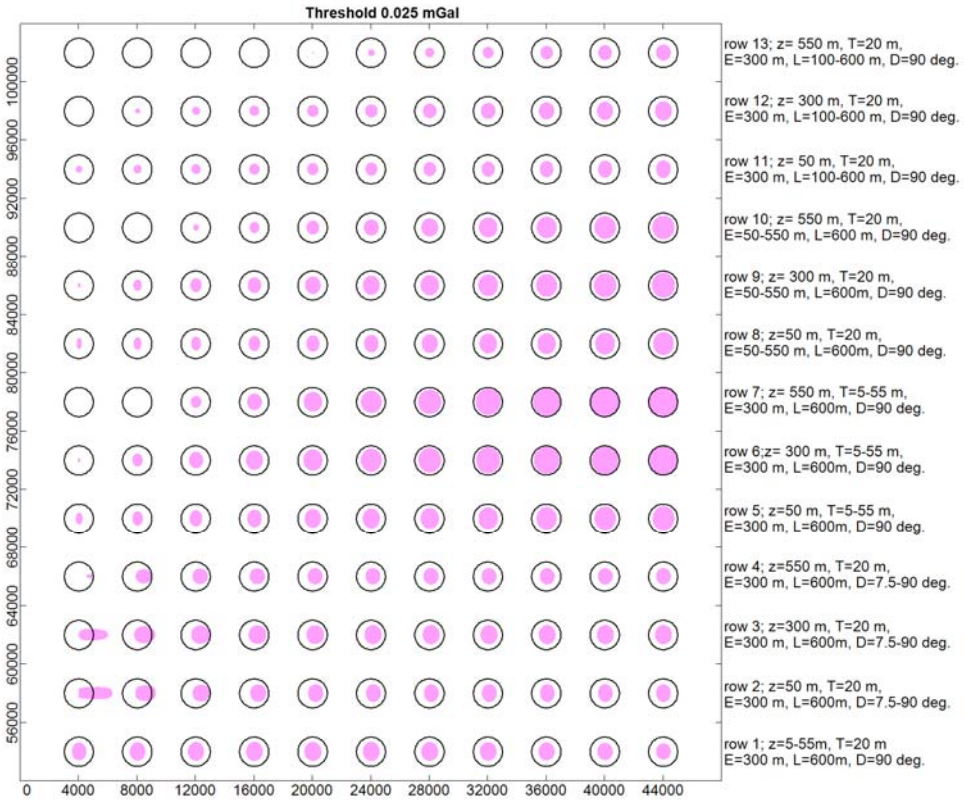

Figure A5. *Thickness 20 m (except rows 5-7) and threshold of 0.025 mGal.*

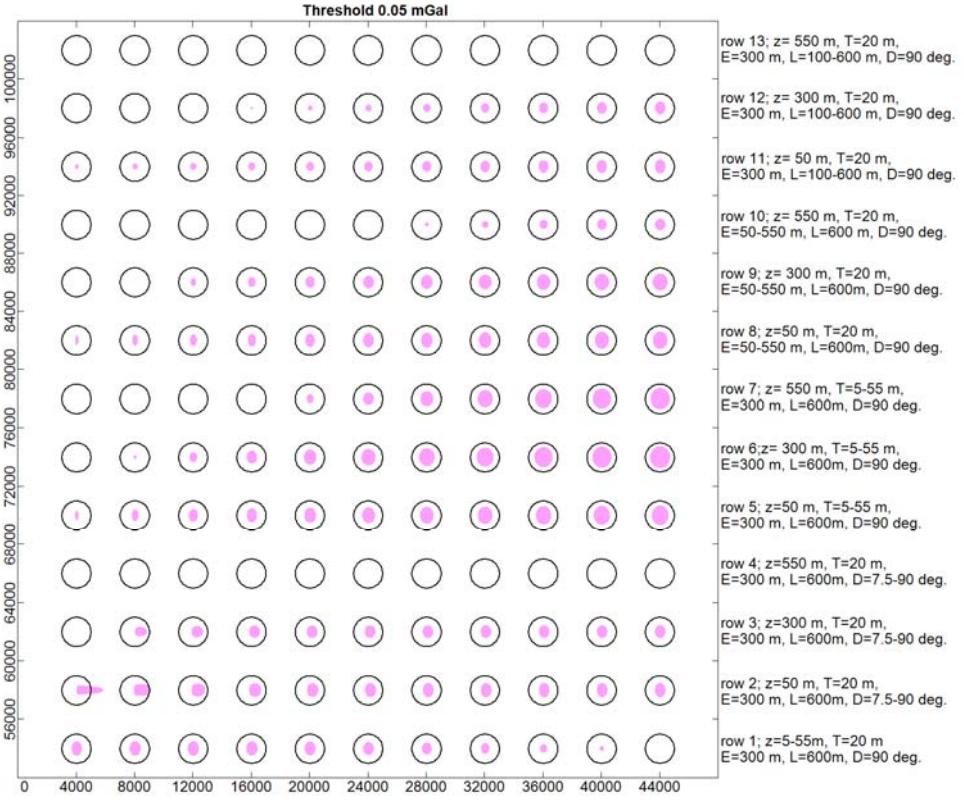

Figure A6. *Thickness 20 m (except rows 5-7) and threshold of 0.05 mGal.*

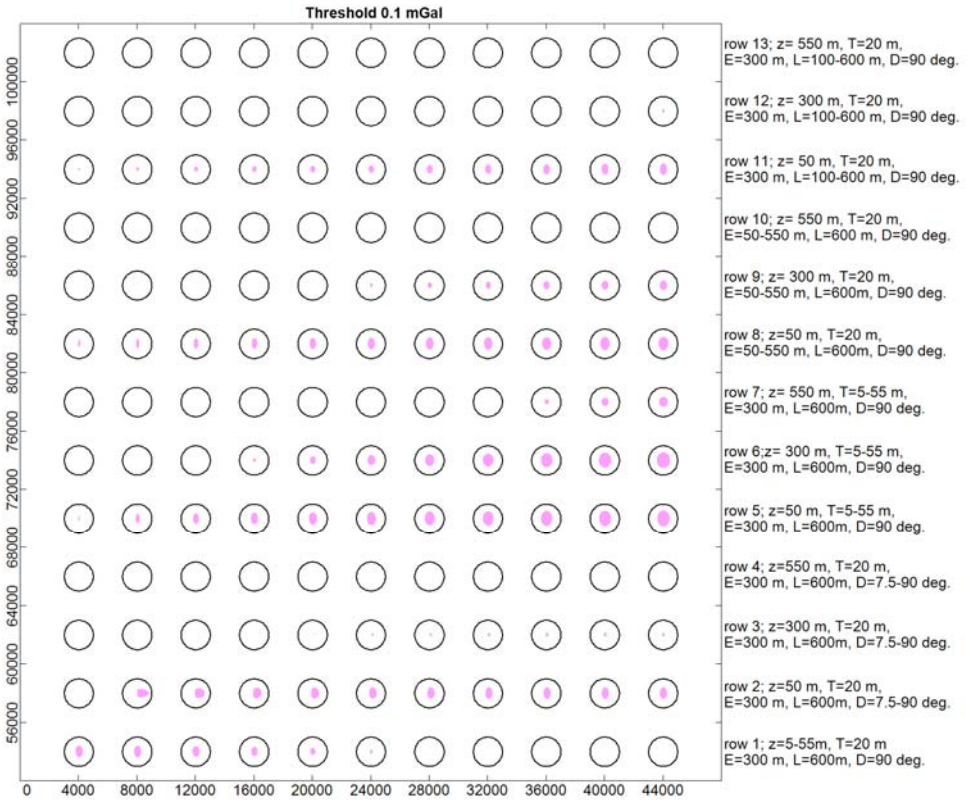

Figure A7. *Thickness 20 m (except rows 5-7) and threshold of 0.10 mGal.*

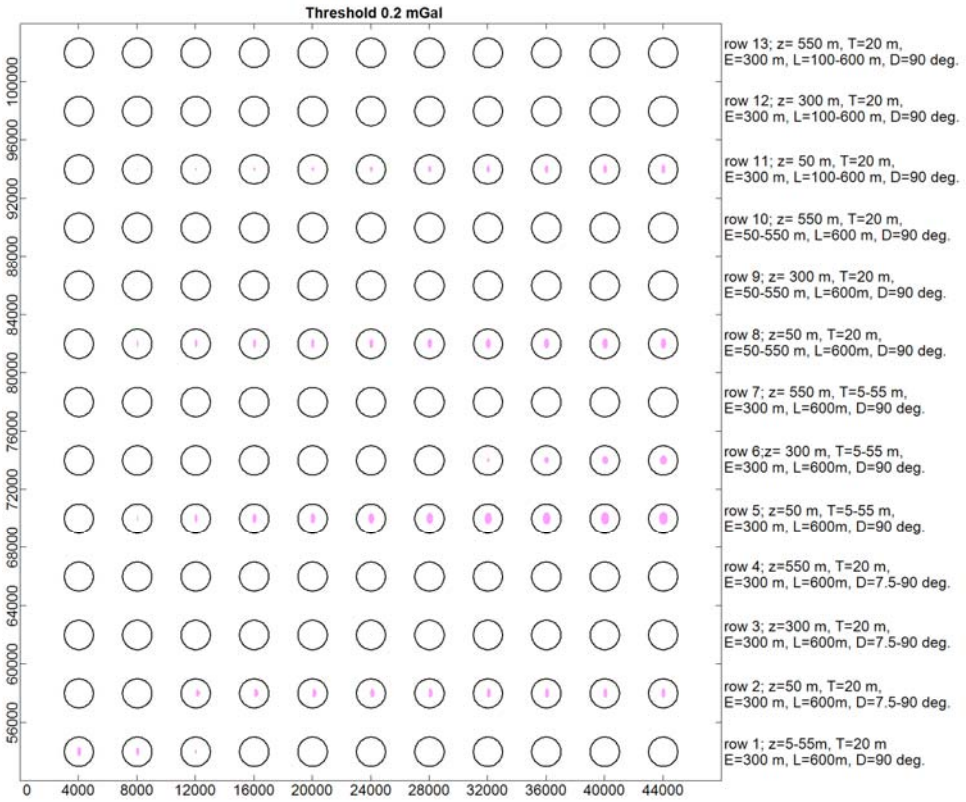

Figure A8. *Thickness 20 m (except rows 5-7) and threshold of 0.20 mGal.*

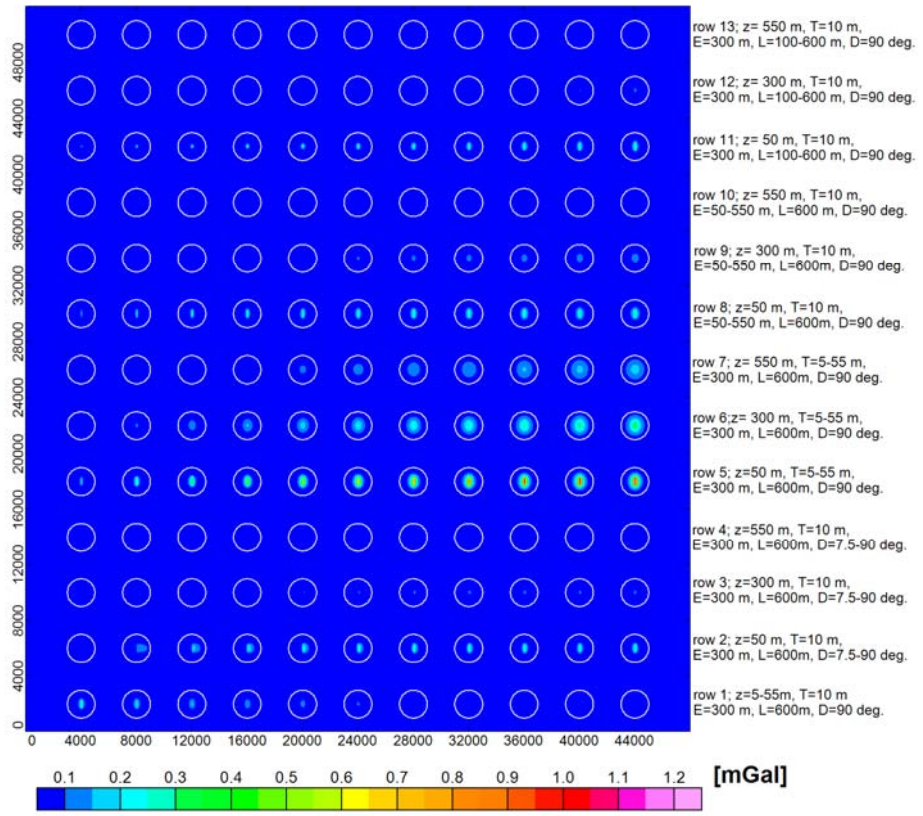

Figure A9. *Thickness 10 m except for rows 5 to 7.*

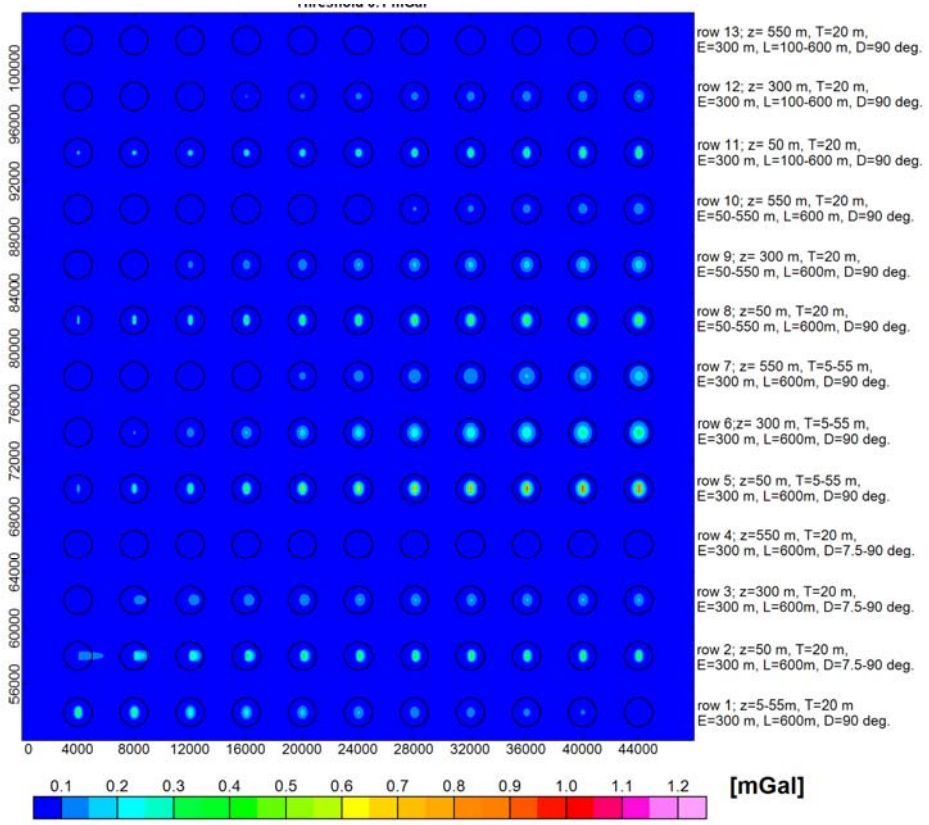

Figure A10. *Thickness 20 m except for rows 5 to 7.*